Supporting Information

Chalcogen-Based Ratiometric Reversible BODIPY Redox Sensors for the Determination of Enantioselective Methionine Sulfoxide Reductase Activity

Michal Poljak,[a,b] Lucie Wohlrábová,[c] Eduardo Palao,[a,b] Jela Nociarová,[a,b] Jiří Míšek,[d] Tomáš Slanina,[c]* Petr Klán[a,b]*

[a] Department of Chemistry, Faculty of Science, Masaryk University, Kamenice 5, 625 00 Brno, Czech Republic. E-mail: klan@sci.muni.cz

[b] RECETOX, Faculty of Science, Masaryk University, Kamenice 5, 625 00 Brno, Czech Republic

[c] Institute of Organic Chemistry and Biochemistry, Flemingovo náměstí 542, 160 00 Prague, Czech Republic. E-mail: tomas.slanina@uochb.cas.cz

[d] Department of Organic Chemistry, Faculty of Science, Charles University in Prague, Hlavova 2030/8, 12843 Prague 2, Czech Republic

Contents

Material and Methods

All experiments were performed with commercially available chemicals in reagent grade from specialized manufacturers (Acros, Lach-ner, Penta, Merck, Sigma Aldrich, Fluorochem). Unless specified otherwise, all reactions were performed under anhydrous conditions under an inert gas atmosphere (nitrogen or argon) and flame-dried or oven-dried glassware.

Dichloromethane and chloroform (Lach-ner) were used without drying over molecular sieves. Dichloromethane was re-distilled before use. Toluene, DMF, and THF (Acros) were purchased as extra dry stored over molecular sieves. Methanol, ethanol (Penta), and acetonitrile (Acros) (HPLC grade) were used as purchased. PBS solutions were prepared from tablets (Sigma Aldrich) to give a 0.1 M solution of phosphate-buffered saline with pH = 7.4 at 25 °C. Degassed solvents were prepared by the freeze-pump-thaw technique over 3 cycles.

Silica gel used for column chromatography was purchased from Merck (pore size 60 Å, 230-400 mesh, particle size 40-63 μm). Reverse silica gel for reverse column chromatography was purchased from Merck (LiChroprep® RP-18, particle size 40-63 μm). Crude products were loaded onto a column either dissolved in the mobile phase or pre-adsorbed on a sufficient amount of Celite®.

Thin-layer chromatography used to monitor the reactions or for purification purposes was performed on silica-coated aluminum or glass plates 60 F_{254} (Merck) or reverse silica (RP-18)-coated aluminum plates 60 $F_{254}S$. The spots were detected by UV light (254 nm or 365 nm) or visualized using basic $KMnO_4$ or PMA solutions.

NMR spectra were measured on a Bruker Avance 500 instrument with the operating frequency of 500 MHz (^{1}H NMR) and 125 MHz (^{13}C NMR) or a Bruker AVANCE 300 instrument with the operating frequency of 300 MHz (^{1}H NMR) at 303 K. The chemical shifts were calibrated in ppm using residual solvent peaks of deuterated solvents $CDCl_3$ (^{1}H NMR: δ = 7.26 ppm; ^{13}C NMR: δ = 77.23 ppm) and CD_3OD (^{1}H NMR: δ = 3.31 ppm; ^{13}C NMR: δ = 49.00 ppm).

IR spectra were measured on a Bruker Alpha Platinum-ATR instrument or a Nicolet 6700 spectrometer (USA) equipped with a standard mid-IR source, a KBr beam-splitter, a DTGS detector, and a cell compartment purged by dry nitrogen. IR spectra were measured in transmission mode in KBr pellets with a diameter of 4 mm in the 4000–400 cm^{-1} range using a

standard experimental setup (the spectral range with a 2 cm^{-1} spectral resolution, Happ–Genzel apodization function, 64 scans).

HRMS spectra were measured on an Agilent 6224 Accurate-Mass TOF LC/MS System in a negative mode using atmospheric-pressure chemical ionization (APCI) or electrospray ionization (ESI) or an FTMS mass spectrometer LTQ-orbitrap XL (Thermo Fisher Scientific) in an electrospray ionization mode.

Melting points were determined on a melting Point Apparatus Stuart SMP 40 and are uncorrected.

HPLC analyses were performed on a DIONEX Ultimate 3000SD device (column: Chiralpak® DAICEL IA, 250 × 4.6 mm, 5 μm) and an Agilent Technologies 1260 Infinity device (columns: NUCLEODEX® alpha-PM, 200 × 4.0 mm, 5 μm; and NUCLEODEX® beta-PM, 200 × 4.0 mm, 5 μm).

Absorption spectra and the molar absorption coefficients were obtained on scanning and diode array UV-vis spectrometers with matched 1.0 cm quartz cells. The sample concentration for absorption spectra was approximately c = 10 μM. Molar absorption coefficients were determined from the absorption spectra (the average value was obtained from three independent measurements with solutions of different concentrations). Fluorescence spectra were recorded on an automated scanning and diode array luminescence spectrometer in 1.0 cm and diode quartz fluorescence cuvettes at 25 ± 1 °C. The sample concentration was set to keep the absorbance at approximately 0.1 at λ_{exc}, *i.e.,* c ~ 5 μM; each sample was measured five times, and the spectra were averaged. Emission and excitation spectra are normalized; they were corrected using standard correction files. The quantum yields of fluorescence were obtained using a calibrated integration sphere or a relative determination using a standard compound with the identical emission spectrum (**1-SOPh** (Φ_{fl} = 0.703 ± 0.002 in MeCN) as a standard for highly emitting samples). Intersystem crossing quantum yields were calculated from the relative ratios of the areas of absorption and ground state bleach bands in the transient spectrum according to our previous studies.[1,2] All spectra were obtained with fresh samples under the same experimental conditions, and the measurements were repeated at least 6 times. The absorbance of 0.1 at the wavelength of excitation was kept to minimize the interference of the ground state absorption. The saturation conditions (quantitative excitation of molecules) were kept for all measurements.

Experimental Part

Monosubstituted compounds **1-SPh, 1-SePh**, and **1-SMe** were synthesized from 6-iodo BODIPY derivative (**3**) using the corresponding tributylstannyl derivative (**4a**, **4b**, and **4c** respectively) and $Pd(PPh_3)_4$ in degassed toluene under argon atmosphere at reflux in 44–63% yields. Disubstituted compound **2-(SPh)(SPh)** was synthesized from 2,6-diiodo BODIPY derivative (**5**) using tributylstannyl derivative **4a** and $Pd(PPh_3)_4$ in degassed toluene under an argon atmosphere at reflux in 87% yield (Scheme S1).

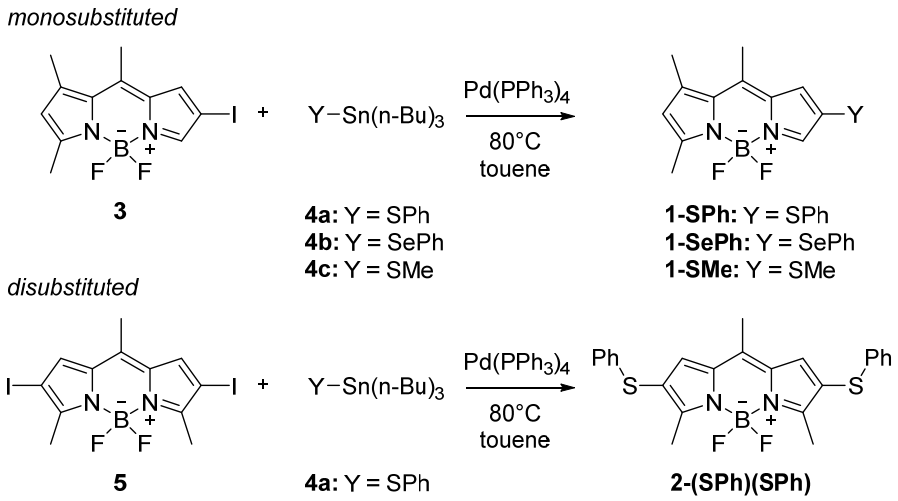

Scheme S1. Synthesis of mono- and dichalcogen-substituted BODIPY derivatives.

The prepared sulfides (**1-SPh, 1-SMe** and **2-(SPh)(SPh)**) and selenide (**1-SePh**) were further oxidized using m-CPBA at 0 °C to obtain sulfoxides (**1-SOPh**, **1-SOMe**, **2-(SOPh)(SPh)**, **2-(SOPh)(SOPh)**) and selenoxide (**1-SeOPh**) (Scheme S2).

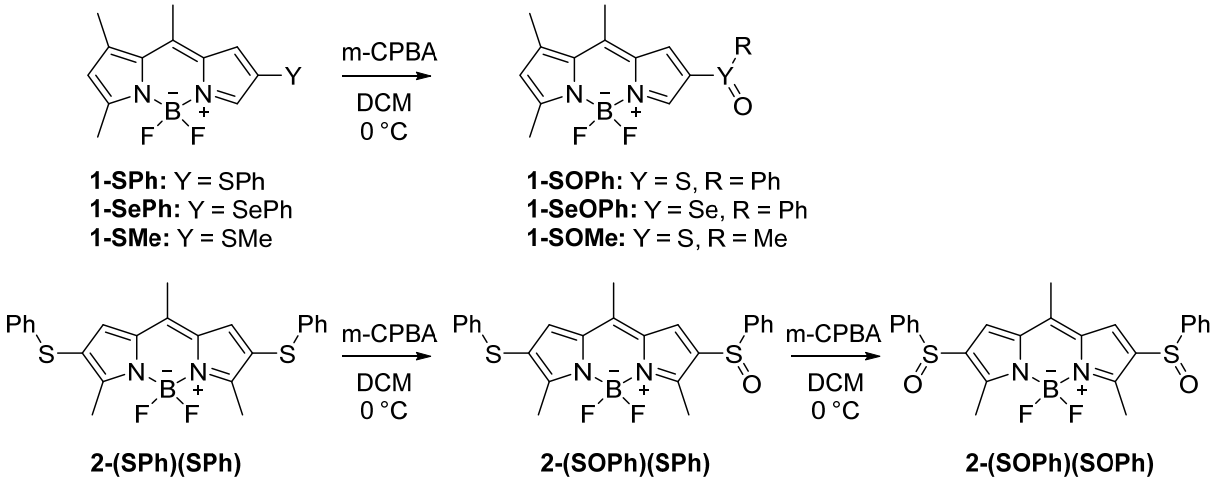

Scheme S2. Synthesis of oxidized of mono- and dichalcogen-substituted BODIPY derivatives.

Water-soluble sulfonic acid **1-(SMe)(SO$_3$)** was prepared by sulfonation[7] of **1-SMe** with an excess of SO$_3$·DMF complex in 25% yield (Scheme S3). The final oxidation of **1-(SMe)(SO$_3$)** to sulfoxide **1-(SOMe)(SO$_3$)** was performed with *m*-CPBA.

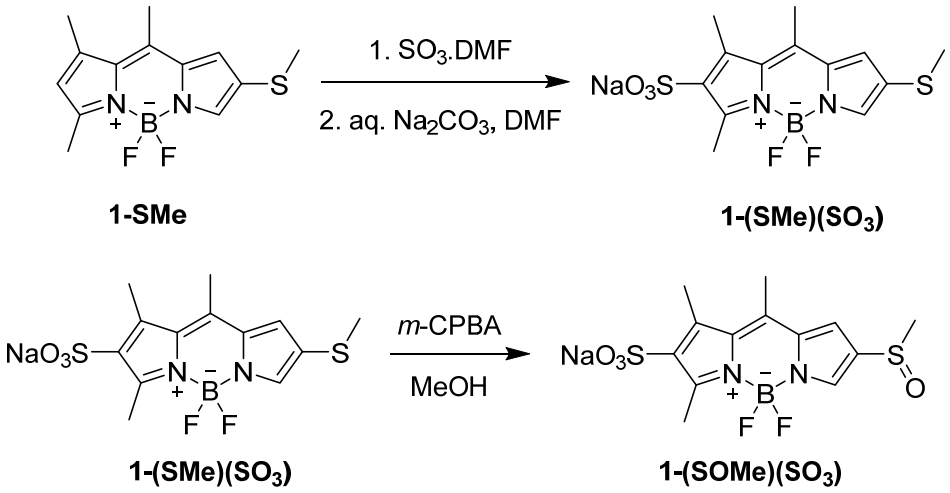

1-SMe **1-(SMe)(SO$_3$)**

1-(SMe)(SO$_3$) **1-(SOMe)(SO$_3$)**

Scheme S3. The synthesis of sulfoxidede **1-(SOMe)(SO$_3$)**.

The resulting racemic mixture of sulfoxides **(*S*)-1-(SOMe)(SO$_3$)** and **(*R*)-1-(SOMe)(SO$_3$)** was resolved into two enantiomers using HPLC (Figure S38). The separation of the racemic mixture of **(*S*)-1-SOMe** and **(*R*)-1-SOMe** was not successful, thus the compound **1-SOMe** was used as a mixture of enantiomers in the subsequent enzymatic analysis.

Compound Characterization

The tributylstannyl compounds **4a-b**,[3–5] iodinated BODIPYs,[6] and BODIPY-selenides and sulfides (**1-SPh, 1-SePh**, **1-SMe, 2-(SPh)(SPh)**)[2] were prepared by reported methods cited below. Selenium-based BODIPY **1-SeOPh** was characterized only spectroscopically because of its thermal instability.

4,4'-Difluoro-1,3,8-trimethyl-6-(methylsulfoxide)-4-bora-3a,4a-diaza-*s*-indacene (1-SOMe).

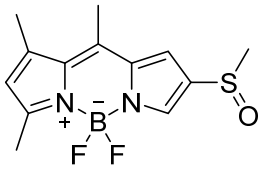

A solution of *m*-chloroperoxybenzoic acid (77%, 41 mg, 0.18 mmol) in dry dichloromethane (5 mL) was added dropwise to a solution of **1-SMe** (47 mg, 0.17 mmol) in dry dichloromethane (10 mL) at 0 °C under nitrogen atmosphere. An immediate color change from red to yellow was observed (TLC in hexane/dichloromethane, 1:1), and after 30 min, the reaction mixture was quenched with saturated aqueous $NaHCO_3$ (10 mL) at 22 °C. The crude mixture was subsequently extracted into dichloromethane (3 × 20 mL), washed with brine, dried with anhydrous $MgSO_4$, filtered, and concentrated to dryness. The crude product was purified by flash column chromatography on silica gel using hexane/ethyl acetate/methanol (5:4:1) to give the product with detectable impurities. The purified product was further recrystallized from pentane to obtain the title compound **1-SOMe** (47 mg, 95 %) as a yellow solid.

Mp. 159−161 °C. ^{1}H NMR (500 MHz, $CDCl_3$, Figure S1): δ (ppm) 7.73 (s, 1H, CH), 7.40 (s, 1H, CH), 6.31 (s, 1H, CH), 2.89 (s, 3H, CH_3), 2.63 (s, 3H, CH_3), 2.62 (s, 3H, CH_3), 2.48 (s, 3H, CH_3). **^{13}C NMR** (125 MHz, $CDCl_3$, Figure S2): δ (ppm) 165.3, 148.5, 141.7, 136.4, 134.6, 133.0, 132.9, 125.2, 118.4, 42.9, 17.3, 16.4, 15.5. **IR** (Figure S3): 3138, 2988, 2926, 1727, 1645, 1567, 1359, 1307, 1154, 1030, 1011, 1096, 1084, 969, 610 cm^{-1}. **HRMS-APCI$^-$** (Figure S4): calcd to $C_{13}H_{14}BF_2N_2OS$ [M – H$^+$] 295.0897, found 295.0896.

4,4'-Difluoro-1,3,8-trimethyl-6-(phenylthio)-4-bora-3a,4a-diaza-*s*-indacene (1-SOPh).

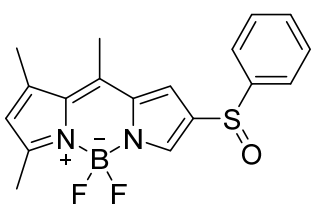

A solution of *m*-chloroperoxybenzoic acid (77%, 7.9 mg, 0.035 mmol) in dry dichloromethane (5 mL) was added dropwise to a solution of (**1-SPh**, 10 mg, 0.029 mmol) in dry dichloromethane (2 mL) at 0 °C under nitrogen atmosphere. An immediate color change from red to yellow was observed (TLC in hexane/dichloromethane, 1:1), and after 30 min, the reaction mixture was quenched with saturated aqueous $NaHCO_3$ (10 mL) at 22 °C. The

crude mixture was subsequently extracted into dichloromethane (3 × 20 mL), washed with brine, dried with anhydrous $MgSO_4$, filtered, and concentrated to dryness. The crude product was purified by flash column chromatography on silica gel using hexane/ethyl acetate/methanol (5:4:1) to give the product with detectable impurities. The purified product was further recrystallized from pentane to obtain the title compound **1-SOPh** (10 mg, 96 %) as a yellow solid.

Mp. 172−174 °C. **^{1}H NMR** (401 MHz, $CDCl_3$, Figure S5) δ 7.65 (s, 1H, CH), 7.22 (m, 4H. CH), 7.13 (m, 2H, CH), 6.23 (s, 1H, CH), 2.60 (s, 3H, CH_3), 2.56 (s, 3H, CH_3), 2.45 (s, 3H, CH_3). **^{13}C NMR** (101 MHz, $CDCl_3$, Figure S6) δ 165.25, 148.42, 144.83, 141.72, 134.84, 134.70, 130.90, 129.33, 127.20, 125.18, 124.77, 119.74, 27.06, 17.33, 16.33, 15.49. **IR** (Figure S7): 3127, 3061, 2956, 2924, 2854, 1575, 1474, 1437, 1307, 1269, 1153, 1085, 1071, 1042, 748 cm^{-1}, **HRMS-ESI$^+$** (Figure S8): calcd to $C_{18}H_{18}ON_2BF_2S$ [M + H^+] 359.11955, found 359.11945.

Sodium 4,4'-Difluoro-1,3,8-trimethyl-6-(methylthio)-4-bora-3a,4a-diaza-*s*-indacenyl-2-sulfonate (1-(SMe)(SO_3)).

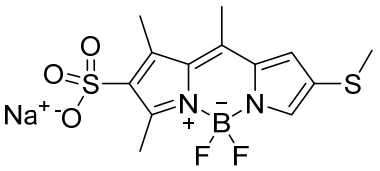

SO_3·DMF complex (141 mg, 0.89 mmol) was added to a stirred solution of **1-SMe** (50 mg, 0.179 mmol) in dry *N*,*N*-dimethylformamide (6 mL) at room temperature under argon atmosphere. The reaction mixture was stirred for 3 h at 60 °C. The reaction was cooled to room temperature after the reaction mixture showed only little presence of the starting material (TLC in hexane/dichloromethane, 1:1) and a major dark red product (TLC in dichloromethane/methanol, 10:1). The reaction mixture was then quenched with saturated aqueous Na_2CO_3 (2 mL), and the reaction was stirred for 30 min at 60 °C. The reaction mixture was then adsorbed on a pad of Celite®. Following the removal of *N*,*N*-dimethylformamide under reduced pressure, the crude product was purified by flash column chromatography on silica gel using dichloromethane/methanol (50:1 to 10:1). The product fraction was concentrated to dryness, re-dissolved in acetonitrile (5 mL), and filtered through a cotton plug to give the title compound **1-(SMe)(SO_3)** (20 mg, 25 %) as a purple solid.

Mp. 286−287 °C. **^{1}H NMR** (500 MHz, MeOD, Figure S9): δ (ppm) 7.60 (s, 1H, CH), 7.31 (s, 1H, CH), 2.78 (s, 3H, CH_3), 2.76 (s, 3H, CH_3), 2.70 (s, 3H, CH_3), 2.44 (s, 3H, CH_3). **^{13}C NMR** (125 MHz, MeOD, Figure S10): δ (ppm) 159.1, 146.0, 144.9, 140.8, 136.7, 136.5, 133.7, 127.3, 126.1, 18.6, 17.8, 15.2, 14.7. **IR** (Figure S11): 2923, 2853, 1563, 1186, 1023, 988, 695, 603,

572 cm^{-1}. **HRMS-ESI$^-$** (Figure S12): calcd to $C_{13}H_{14}BF_2N_2O_3S_2$ [M – Na^+] 359.0515, found 359.0511.

Sodium 4,4'-Difluoro-1,3,8-trimethyl-6-(methylsulfoxide)-4-bora-3a,4a-diaza-*s*-indacenyl-2-sulfonate (1-(SOMe)(SO_3)).

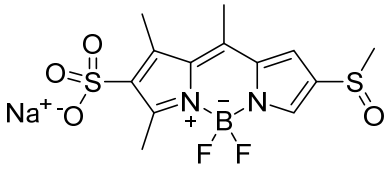

A solution of *m*-chloroperoxybenzoic acid (77%, 8 mg, 0.04 mmol) in methanol (2 mL) was added dropwise to a solution of **1-(SMe)(SO_3)** (13 mg, 0.03 mmol) in methanol (3 mL) at 0 °C under nitrogen atmosphere. An immediate color change from red to yellow was observed (TLC in dichloromethane/methanol, 6:1), and after 30 min, the reaction mixture was concentrated to dryness. The crude product was purified by flash column chromatography on reverse silica gel using methanol/water (2:3) and on normal-phase silica gel using dichloromethane/methanol (6:1) to give the title compound **1-(SOMe)(SO_3)** (12 mg, 92 %) as a yellow solid. **Mp.** 289−290 °C. **^{1}H NMR** (500 MHz, MeOD, Figure S13): δ (ppm) 7.93 (s, 1H, CH), 7.68 (s, 1H, CH), 2.96 (s, 3H, CH_3), 2.85 (s, 3H, CH_3), 2.81 (s, 3H, CH_3), 2.78 (s, 3H, CH_3). **^{13}C NMR** (125 MHz, MeOD, Figure S14): δ (ppm) 164.8, 148.0, 147.0, 139.0, 136.4, 136.0, 135.6, 132.9, 121.0, 41.7, 17.5, 15.5, 15.2. **IR** (Figure S15): 3439, 3119, 3016, 2929, 1566, 1215, 1062, 1023, 990, 683, 600, 571 cm^{-1}. **HRMS-ESI$^-$** (Figure S16): calcd to $C_{13}H_{14}BF_2N_2O_4S_2$ [M – Na^+] 375.0464, found 375.0462.

4,4'-Difluoro-2-(phenylthio)-6-(phenylsulfoxide)-1,5,8-trimethyl-4-bora-3a,4a-diaza-*s*-indacene. (2-(SOPh)(SPh))

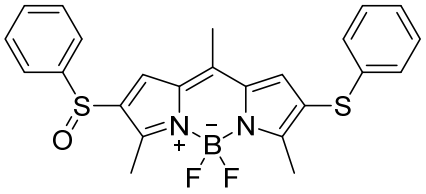

A *m*-chloroperoxybenzoic acid (77%, 5.8 mg, 0,026 mmol, 1.1 eq) solution in anhydrous DCM was dropwise added to an ice-cold solution of **2-(SPh)(SPh)** (10.7 mg, 0.024 mmol, 1 eq) in anhydrous dichloromethane. The reaction was monitored with TLC (cyclohexane/ethyl acetate/methanol – 5/4/1, v/v). The reaction was stirred for 30 min and then quenched with a saturated solution of K_2CO_3. The organic layer was transferred with a syringe to the round bottom flask and evaporated with Celite®. The crude product was purified by flash column chromatography using cyclohexane/ethylacetate/methanol (5/4/1, v/v) as a mobile phase. Then, the solvent was removed, and the solid was dissolved in a small amount of dichloromethane and precipitated with cyclohexane. The liquid part was removed with a syringe, and the solid was dried under reduced pressure to give **2-(SOPh)(SPh)** (7.6 mg, 69 %) as a dark violet solid.

Mp. 164-165 °C. **^{1}H NMR** (400.13 MHz, $CDCl_3$, Figure S17): δ (ppm 7.66 (m, 2H), 7.51 (m, 3H), 7.34 (s, 1H), 7.28 (m, 2H), 7.20 (m, 4H), 2.66 (s, 3H), 2.56 (s, 3H). **^{13}C NMR** (100.62 MHz, CDCl3, Figure S18): 13163.48, 153.24, 144.20, 141.67, 135.50, 135.23, 133.39, 133.16, 130.87, 129.37, 129.31, 128.24, 126.63, 124.74, 124.11, 77.03, 29.72, 26.93, 15.68, 13.29, 12.98 ppm. **IR** (Figure S19): 3056, 2924, 2853, 1632, 1585, 1476, 1460, 1294, 1254, 1106, 1041, 890, 836, 748, 742, 695 cm^{-1}. **HRMS-ESI$^+$** (Figure S20): calcd to $C_{24}H_{22}ON_2BF_2S_2$ [M – H^+] 467.12292, found 467.12254.

4,4'-Difluoro-2,6-di(phenylsulfoxide)-1,5,8-trimethyl-4-bora-3a,4a-diaza-s-indacene (2-(SOPh)(SOPh))

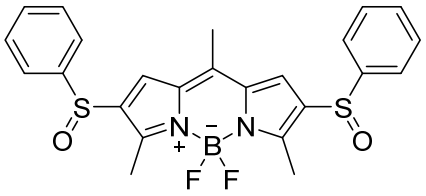

A *m*-chloroperoxybenzoic acid (77%, 10.9 mg, 0,048 mmol, 2 eq) solution in anhydrous dichlorometane was dropwise added to an ice-cold solution of **2-(SPh)(SPh)** (11 mg, 0.024 mmol, 1 eq) in anhydrous dichlorometane. The reaction was monitored with TLC (cyclohexane/ethylacetate/methanol – 5/4/1). A reaction mixture was stirred for 30 min and then quenched with a saturated solution of K_2CO_3. The organic layer was transferred with a syringe to the round bottom flask and evaporated with Celite®. The crude product was purified by flash column chromatography using a cyclohexane/ethylacetate/methanol (5/4/1) mobile phase. Then, the solvent was removed, and the solid was dissolved in a small amount of dichloromethane and precipitated with cyclohexane. The liquid was removed with a syringe, and the solid was dried under reduced pressure to give **2-(SOPh)(SOPh)** (11 mg, 68 %) as a dark brown solid.

Mp. 166-167 °C. **^{1}H NMR** (401 MHz, CDCl3, Figure S21) δ 7.65 (m, 8H, CH), 7.53 (m, 12H, CH), 7.37 (s, 2H, CH), 7.35 (s, 2H, CH), 2.63 (s, 6H, CH_3), 2.61 (s, 6H, CH_3), 2.49 (s, 3H, CH_3), 2.47 (s, 3H, CH_3). **^{13}C NMR** (101 MHz, CDCl3, Figure S22) δ 156.67, 145.11, 145.04, 143.33, 135.51, 135.31, 134.54, 134.39, 133.60, 133.24, 131.52, 131.48, 129.73, 129.66, 129.64, 129.56, 127.37, 127.25, 125.09, 125.02, 29.84, 27.05, 16.03, 13.52. **IR** (Figure S23): 3057, 2965, 2924, 1632, 1572, 1469, 1376, 1262, 1155, 1041, 887, 839, 689 cm^{-1}. **HRMS-ESI$^+$** (Figure S24): calcd to $C_{24}H_{22}O_2N_2BF_2S_2$ [M – H^+] 505.09978, found 505.09994.

Chiral Separation of a Racemic Mixture of (*S*)-1-SOMe and (*R*)-1-SOMe. This racemic mixture was successfully resolved into two enantiomers **(*S*)-1-SOMe** (94% *ee*, the other analyte was the (*R*)-enantiomer) and **(*R*)-1-SOMe** (100% *ee*) by HPLC using a Chiralpak® IA column

as a stationary phase and a mixture of acetonitrile and ethanol (97.5:2.5) as a mobile phase, both in analytical and semi-preparative modes (Figure S38).

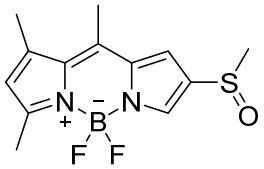

Enzyme Assay for (*S*)-1-SOMe. The title compound (5.0 mg) was dissolved in acetonitrile (500 μL, the concentration of a stock solution: $c = 33.8 \times 10^{-3}$ M). For each of 5 samples, one portion (50 μL) was added to a PBS solution (689 μL; 8% acetonitrile in PBS) containing dithiothreitol with the final concentration of $c = 23.0 \times 10^{-3}$ M. Dithiothreitol was used as a substitute for thioredoxin system to reduce the enzyme to its active form. The samples were then incubated with MsrA (11 μL, 242 μg) against a control (storage buffer of MsrA, 50 mM Tris-HCl buffer, pH 8.0, 11 μL) at 37 °C for 210 min. The final concentration of the probe was $c = 2.3 \times 10^{-3}$ M in 8% acetonitrile in PBS, and the final concentration of MsrA was $c = 6.7 \times 10^{-6}$ M (0.29 mol. % of MsrA based on 100 mol. % of the title compound). In general, MsrA can tolerate up to approximately 10% of acetonitrile in aqueous buffers (acetonitrile was used to increase the solubility of the probes).[10] Each sample was then quenched with acetonitrile to denature the enzyme, extracted to ethyl acetate, and evaporated to dryness. The fluorescence of the samples was recorded after work-up and dilution of the probe to a concentration with approximately $A = 0.1$ (approx. $c = 5 \times 10^{-6}$ M, Figures S39–41). The opposite (*R*)-enantiomer was elaborated in the same way. Control experiments of both **(*S*)-1-SOMe** and **(*R*)-1-SOMe** (in storage buffer without MsrA) provided no decrease in fluorescence.

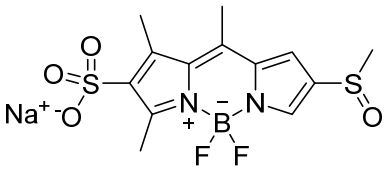

Enzyme Assay for *rac*-1-(SOMe)(SO_3). The title compound (1.3 mg) was dissolved in PBS (100 μL, concentration of stock solution: $c = 33.8 \times 10^{-3}$ M) and added (50 μL) to a PBS solution (689 μL) containing dithiothreitol (the final concentration, $c = 23.0 \times 10^{-3}$ M), resulting in two samples. Dithiothreitol was used as a substitute for the thioredoxin system to reduce the enzyme to its active form. The samples were then incubated with MsrA (11 μL, 242 μg) against the control (storage buffer without MsrA, 11 μL) at 37 °C for 180 min. The final concentration of the probe was $c = 2.3 \times 10^{-3}$ M in PBS, and the final concentration of MsrA was $c = 6.7 \times 10^{-6}$ M (0.29 mol. % of MsrA based on 100 mol. % of the title compound). Every 15 min, a sample (12 μL) from the probe solution with MsrA was transferred to a cuvette with PBS (1888 μL), and the final volume of the analyzed sample was 2.0 mL. For the control experiment, a sample (12 μL) from the probe solution with storage buffer was transferred to a cuvette with PBS (1888 μL) every 90 min. The fluorescence

of the samples was recorded after diluting the probe to a concentration of approximately $A = 0.1$ (approx. $c = 5 \times 10^{-6}$ M, Figures S42–44). The control experiments of ***rac*-1-(SOMe)(SO_3)** without MsrA provided no decrease in fluorescence (Figure S46).

Photophysical Properties

Table S1. Photophysical properties of sulfide **1-SMe**, sulfoxide **1-SOMe**, sulfide **1-(SMe)(SO$_3$)** and sulfoxide **1-(SOMe)(SO$_3$)**.[a]

Compound	λ_{max}(abs)/nm	ε_{max}(abs)/ M^{-1} cm^{-1}	λ_{max}(f)/nm	$\Delta\tilde{\nu}$/cm^{-1}	Φ_F	τ_F/ns	Φ_{ISC}	Solvent
1-SMe	490	25500	638	4734	0.022 ± 0.002	negligible	0.14 ± 0.01	MeCN
1-SOMe	472	31900	505	1385	0.560 ± 0.002	4.29 ± 0.01	0.17 ± 0.02	MeCN
1-(SMe)(SO$_3$)	500	24800	628	4076	0.180 ± 0.001	n.d.	n.d.	MeCN
1-(SMe)(SO$_3$)	497	25400	663	5038	0.006 ± 0.001	n.d.	n.d.	PBS
1-(SOMe)(SO$_3$)	481	31000	515	1372	0.745 ± 0.003	n.d.	n.d.	MeCN
1-(SOMe)(SO$_3$)	476	33100	501	1049	0.385 ± 0.004	n.d.	n.d.	PBS

[a] n.d. = not determined, MeCN = acetonitrile.

All prepared derivatives were stable in acetonitrile, methanol, and PBS solutions for more than a week without any measurable changes in their absorption or emission properties.

Spectra

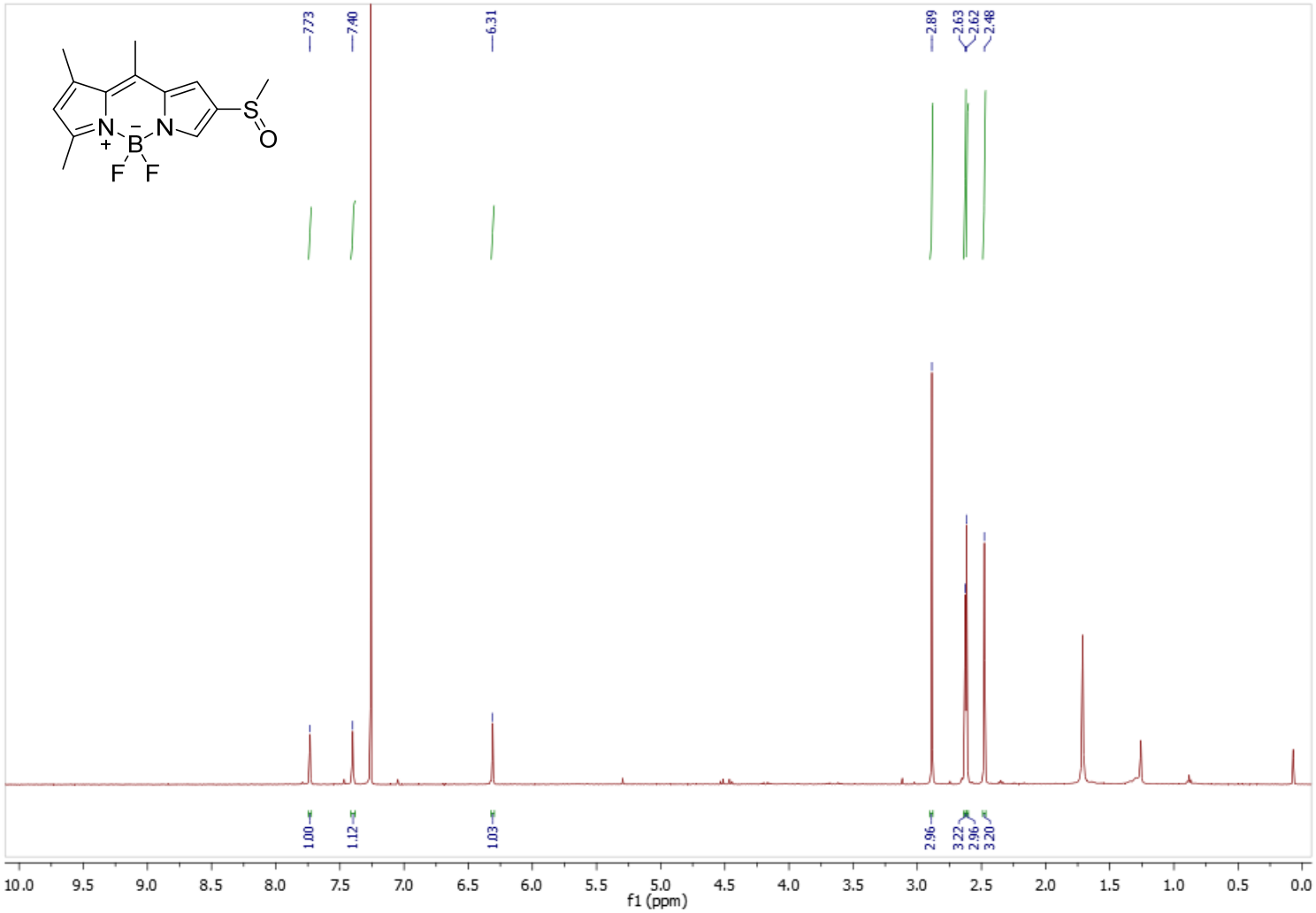

Figure S1. ^{1}H NMR of **1-SOMe** in $CDCl_3$.

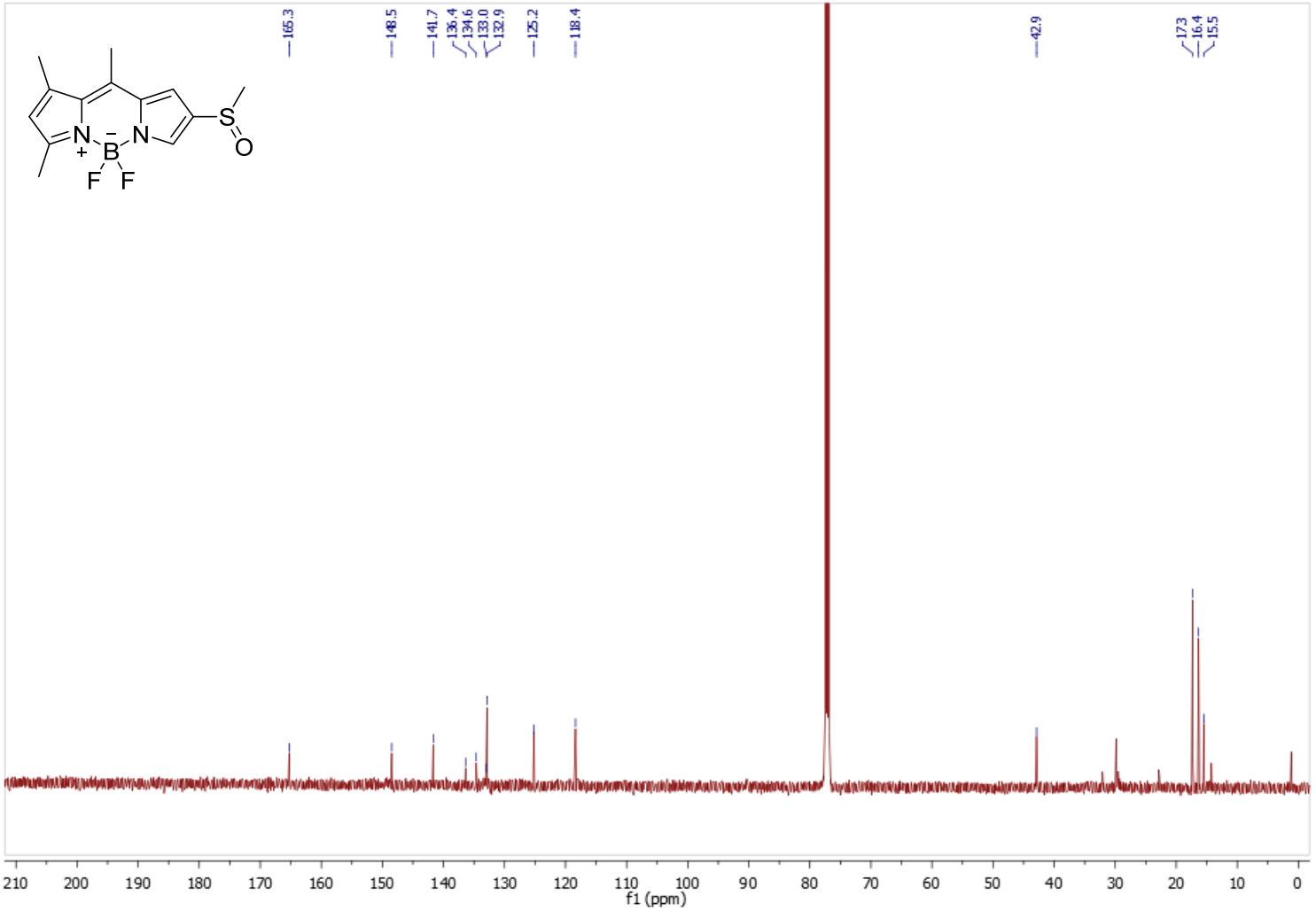

Figure S2. ^{13}C NMR of **1-SOMe** in $CDCl_3$.

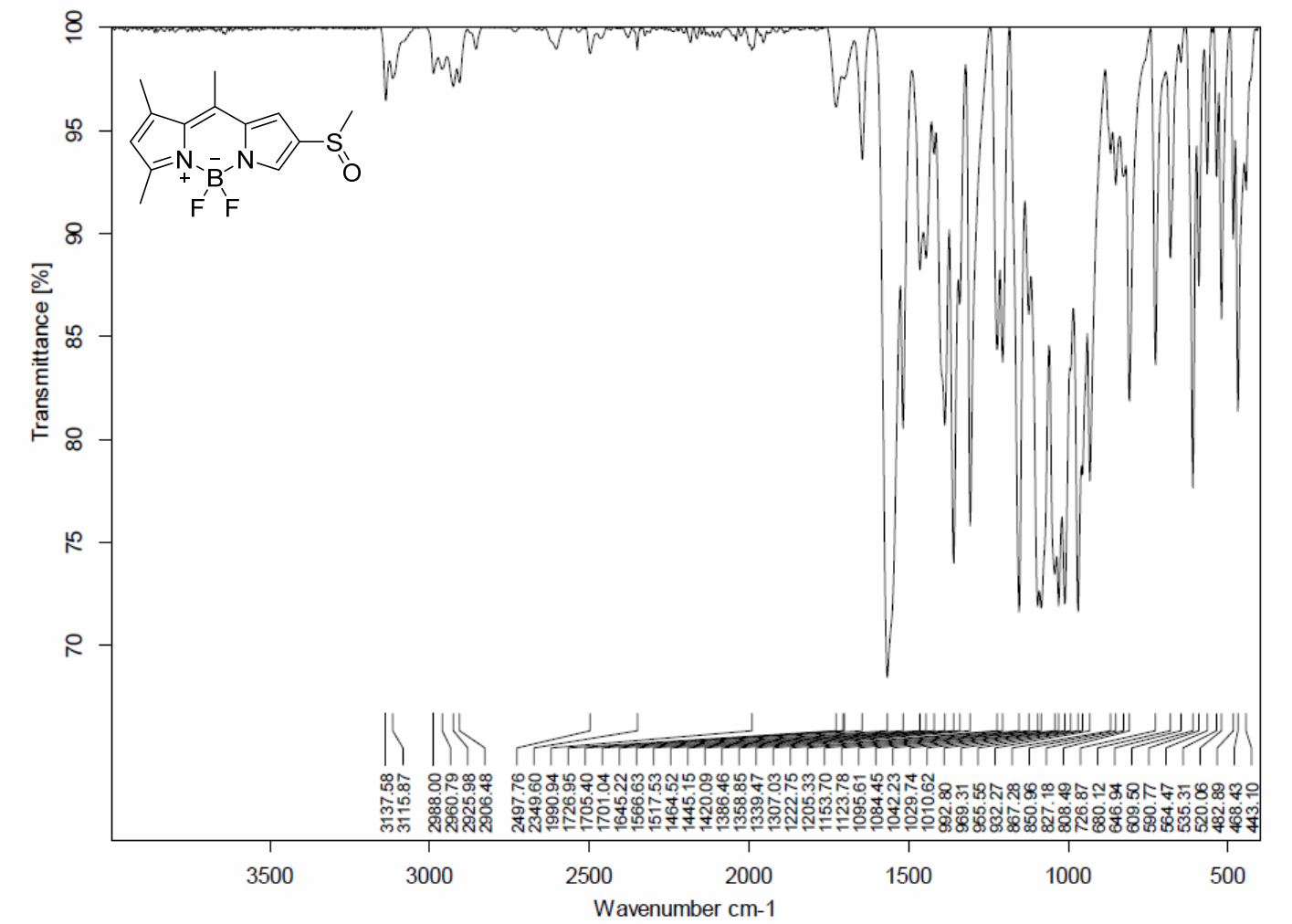

Figure S3. FTIR spectrum of **1-SOMe**.

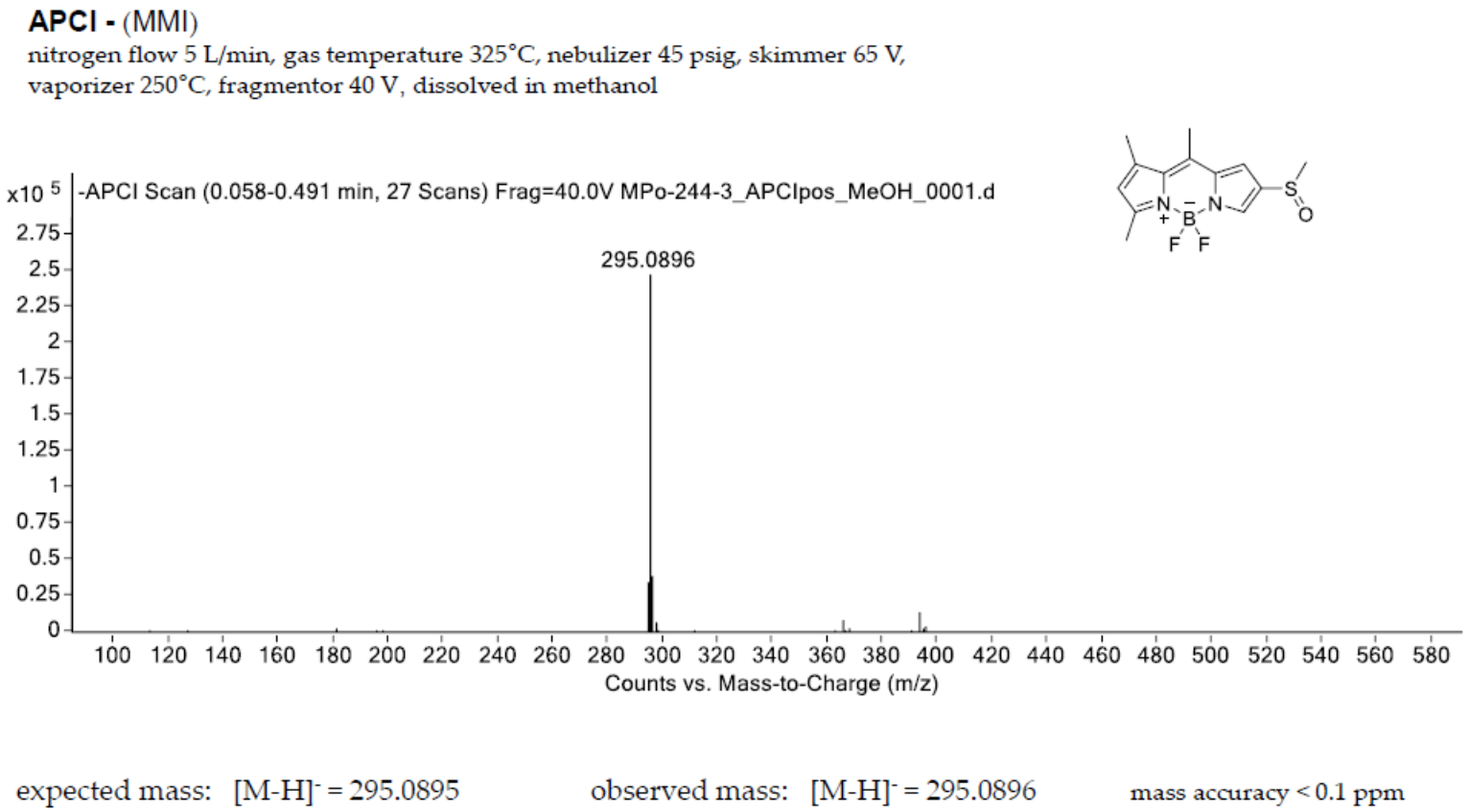

Figure S4. HRMS (APCI) spectrum of **1-SOMe**.

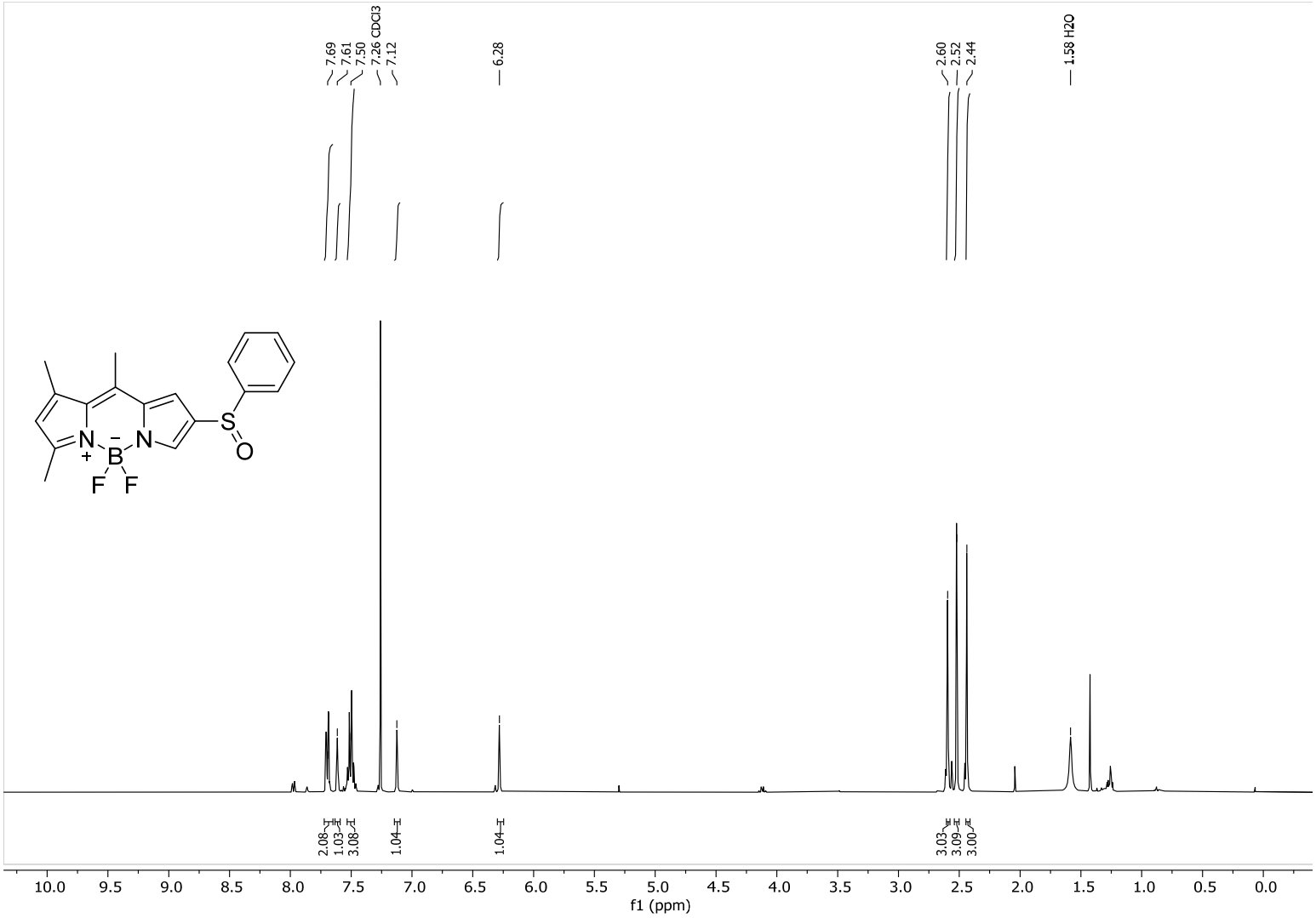

Figure S5. ^{1}H NMR of **1-SOPh** in $CDCl_3$.

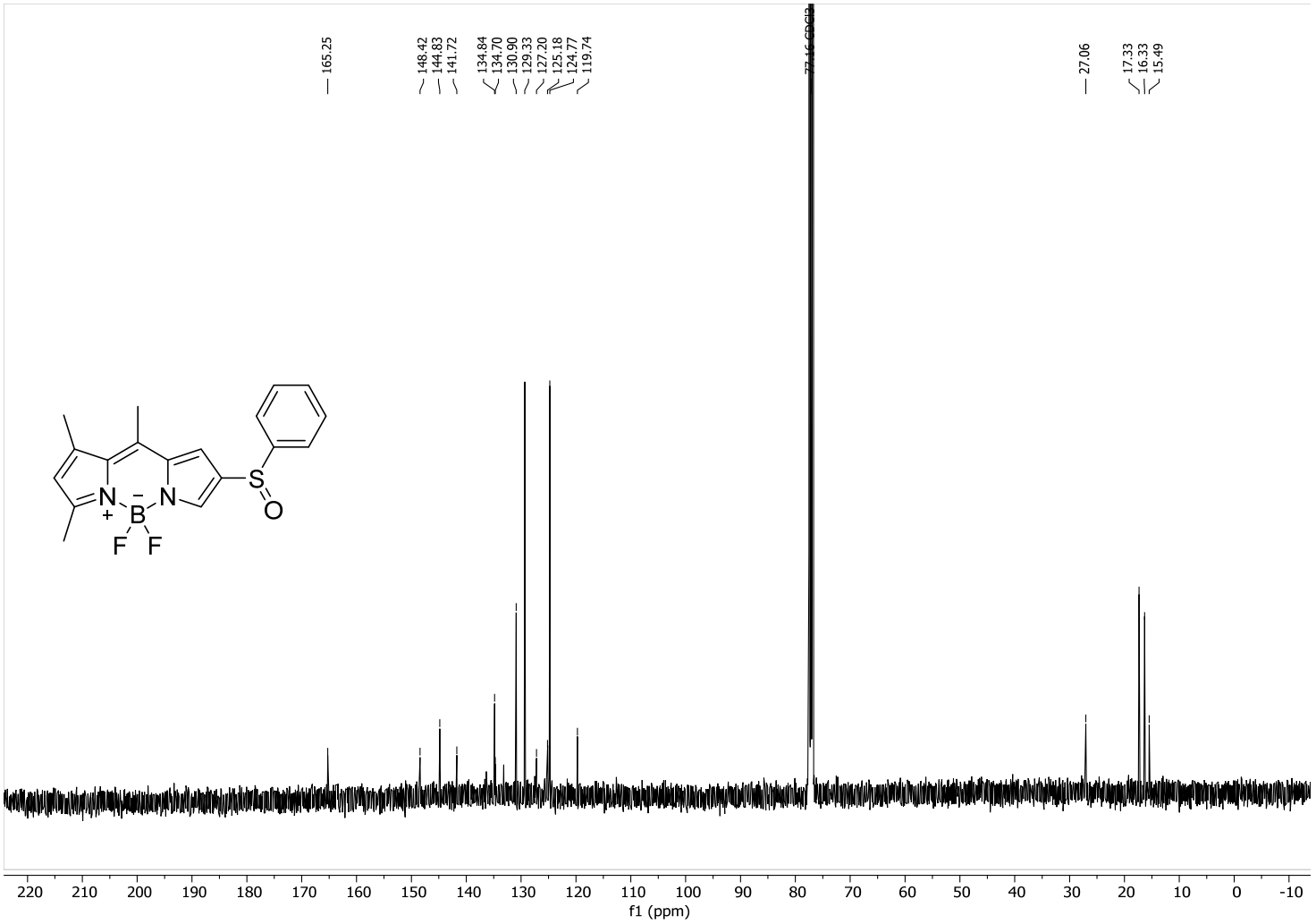

Figure S6. ^{13}C NMR of **1-SOPh** in $CDCl_3$.

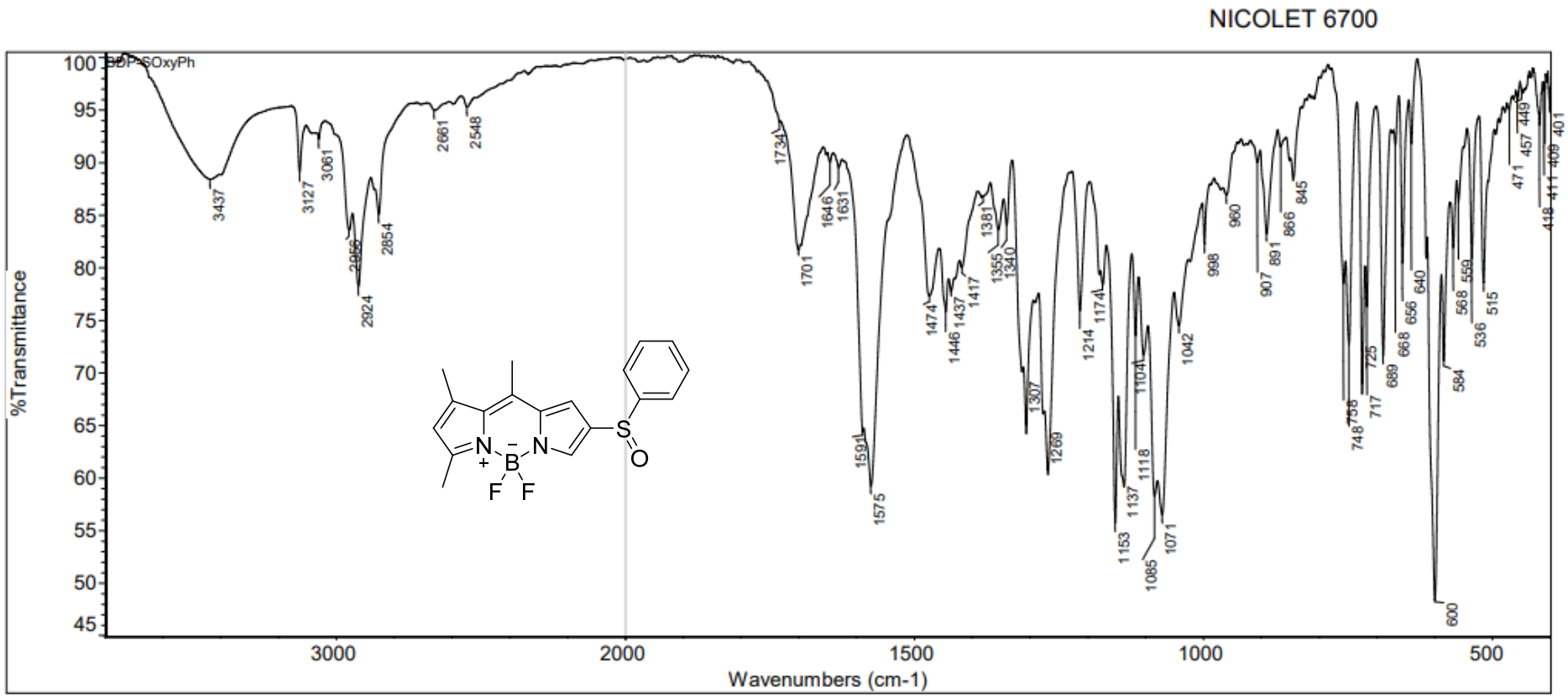

Figure S7. FTIR spectrum of **1-SOPh**.

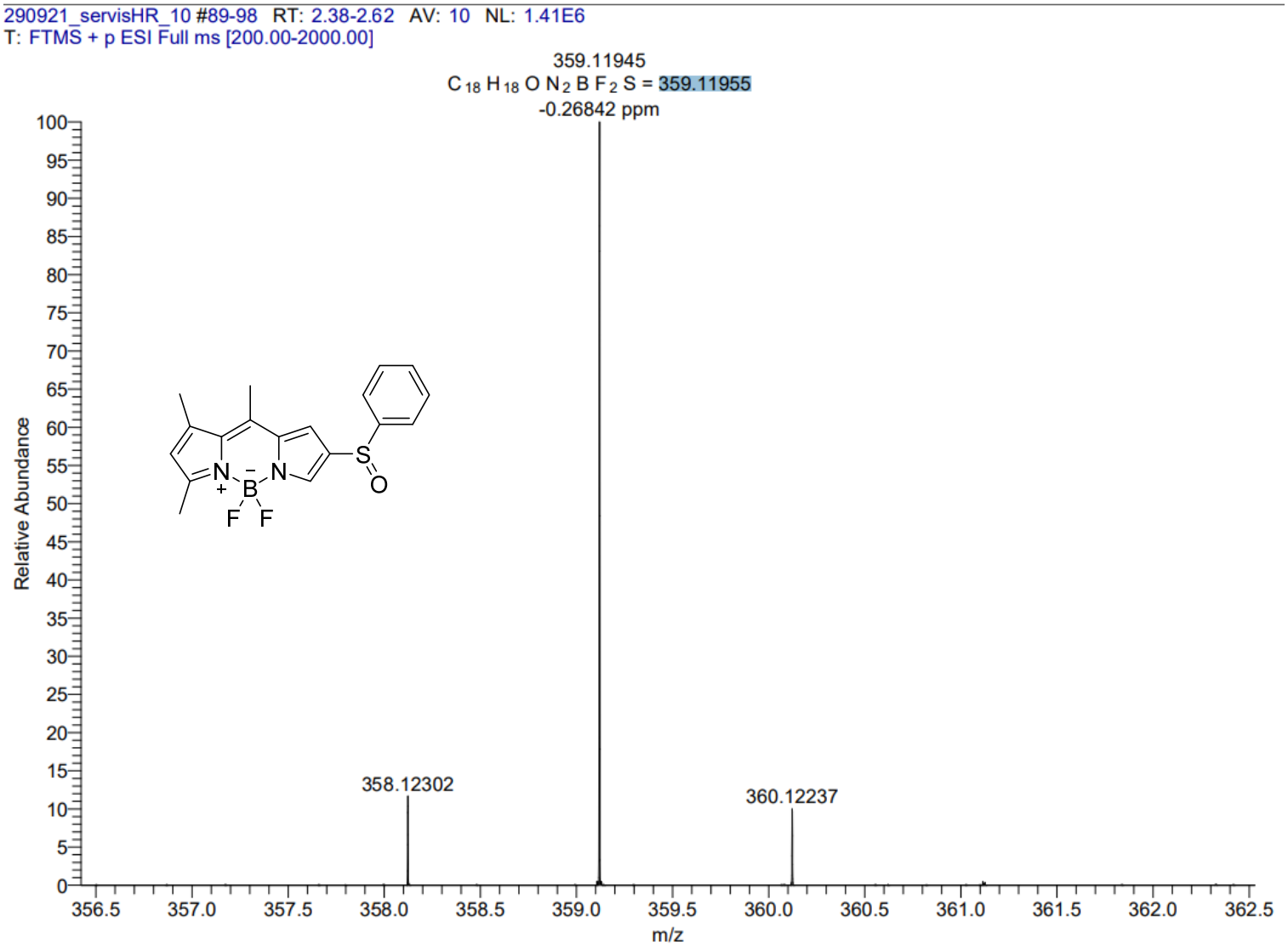

Figure S8. HRMS (ESI+) spectrum of **1-SOPh**.

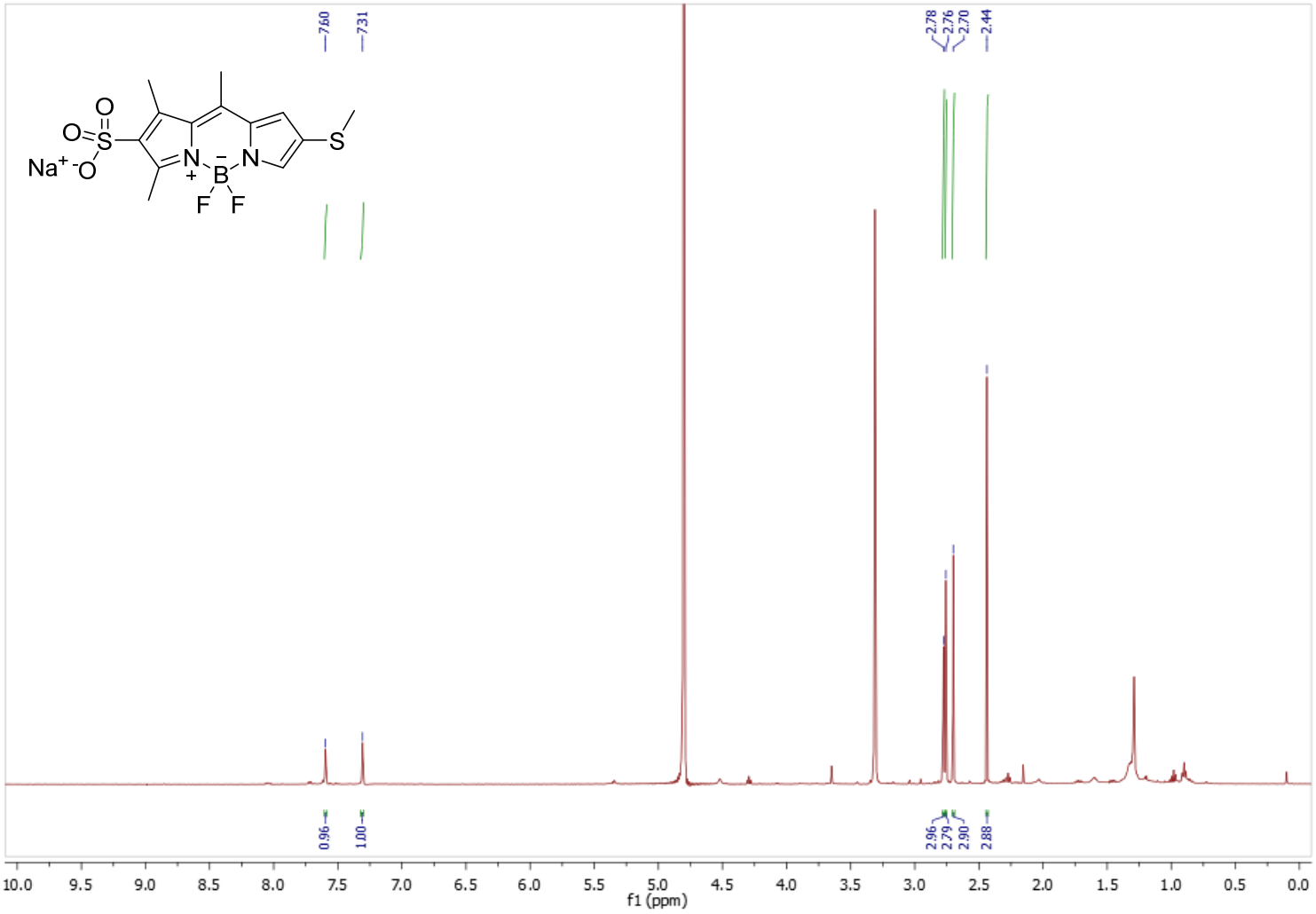

Figure S9. ^{1}H NMR of **1-(SMe)(SO$_3$)** in CD$_3$OD.

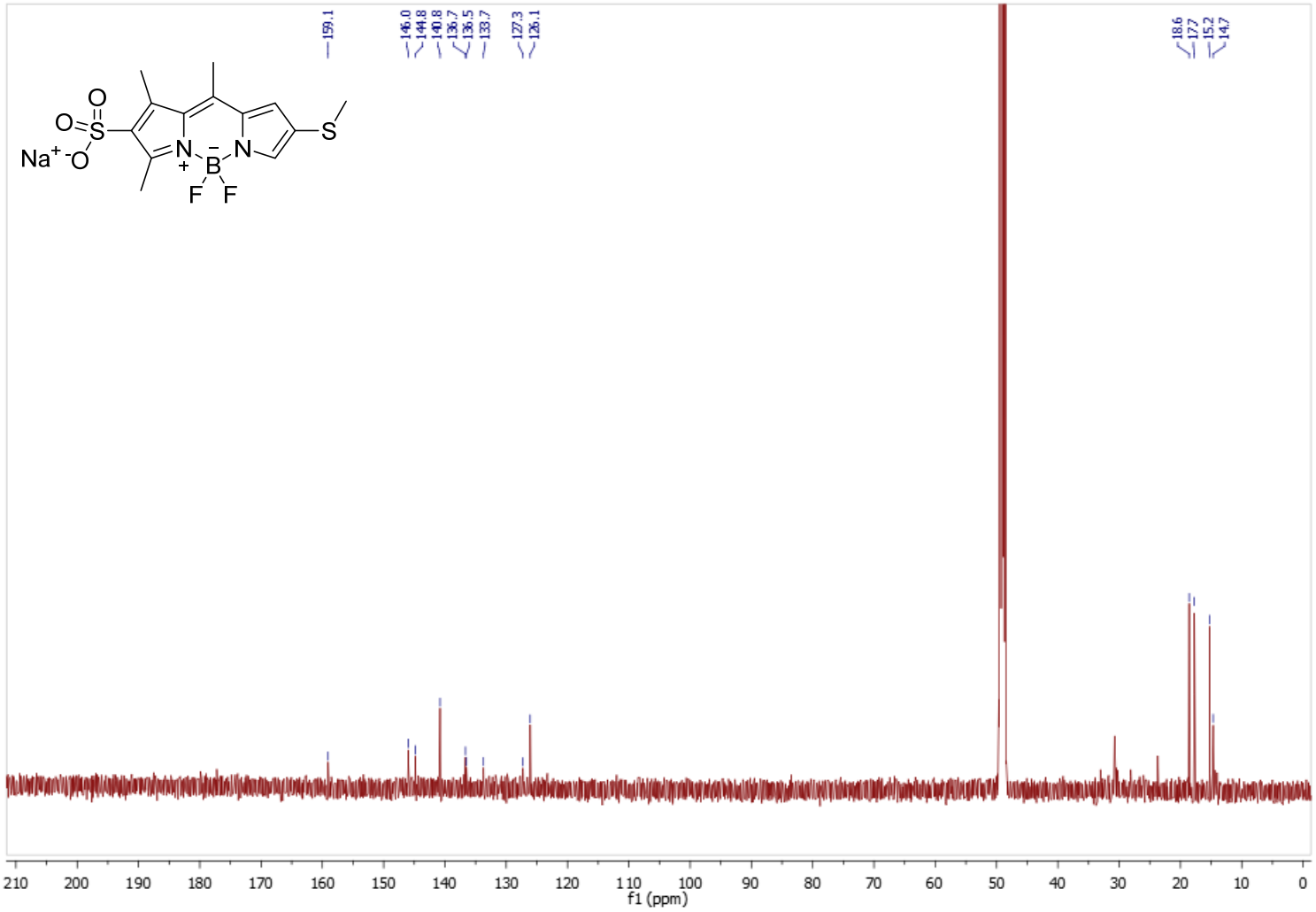

Figure S10. ^{13}C NMR of **1-(SMe)(SO_3)** in CD_3OD.

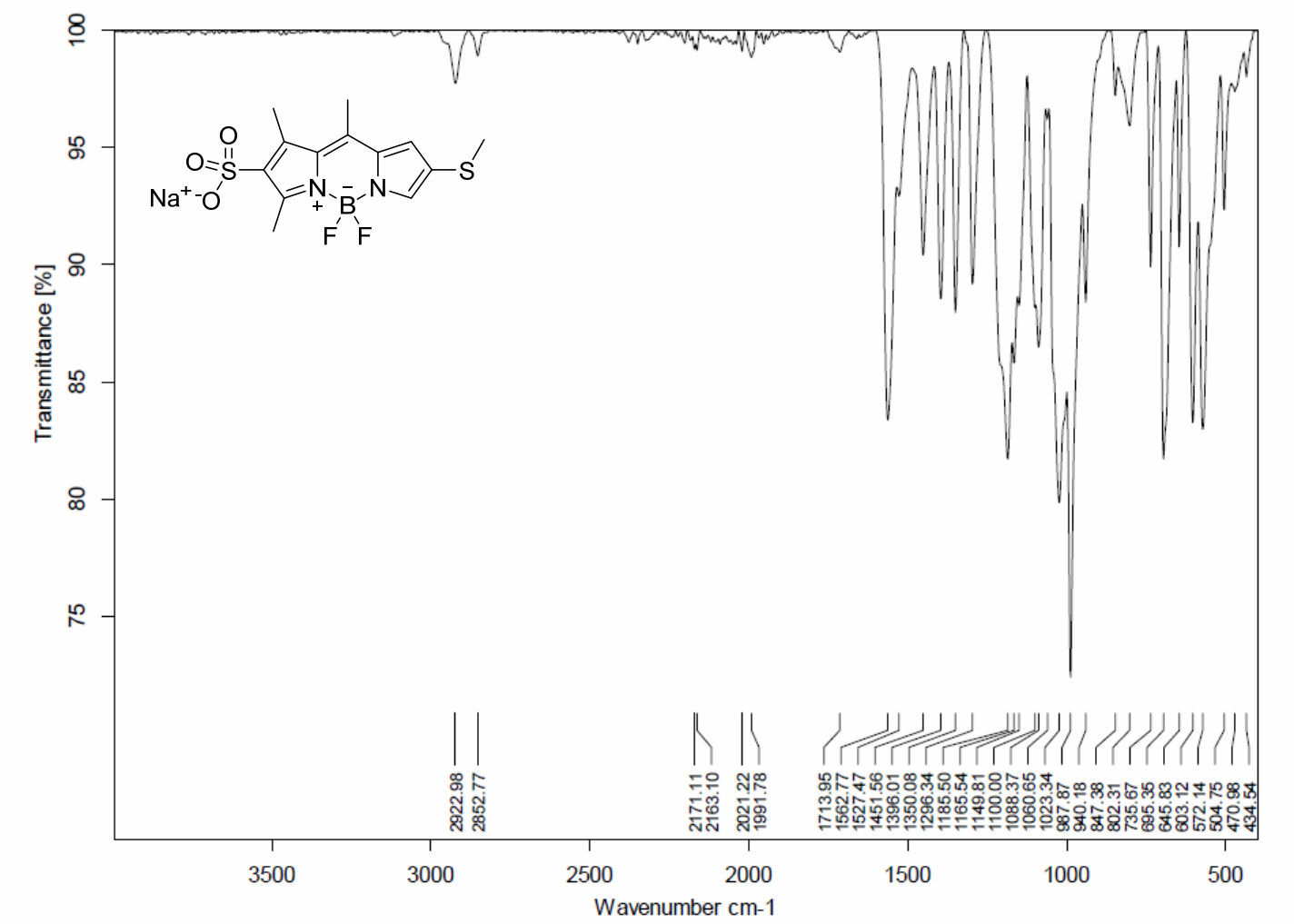

Figure S11. FTIR spectrum of **1-(SMe)(SO_3)**.

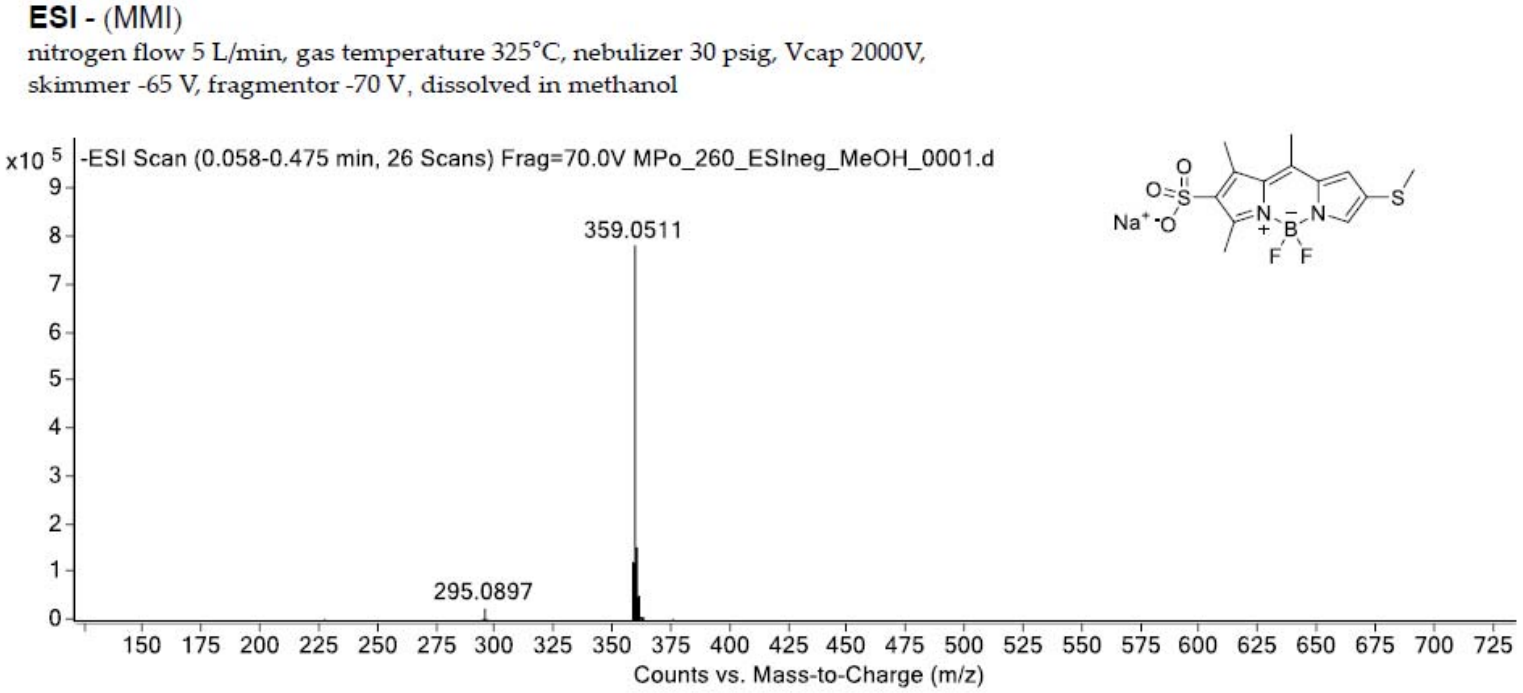

Figure S12. HRMS (ESI-) spectrum of **1-(SMe)(SO_3)**.

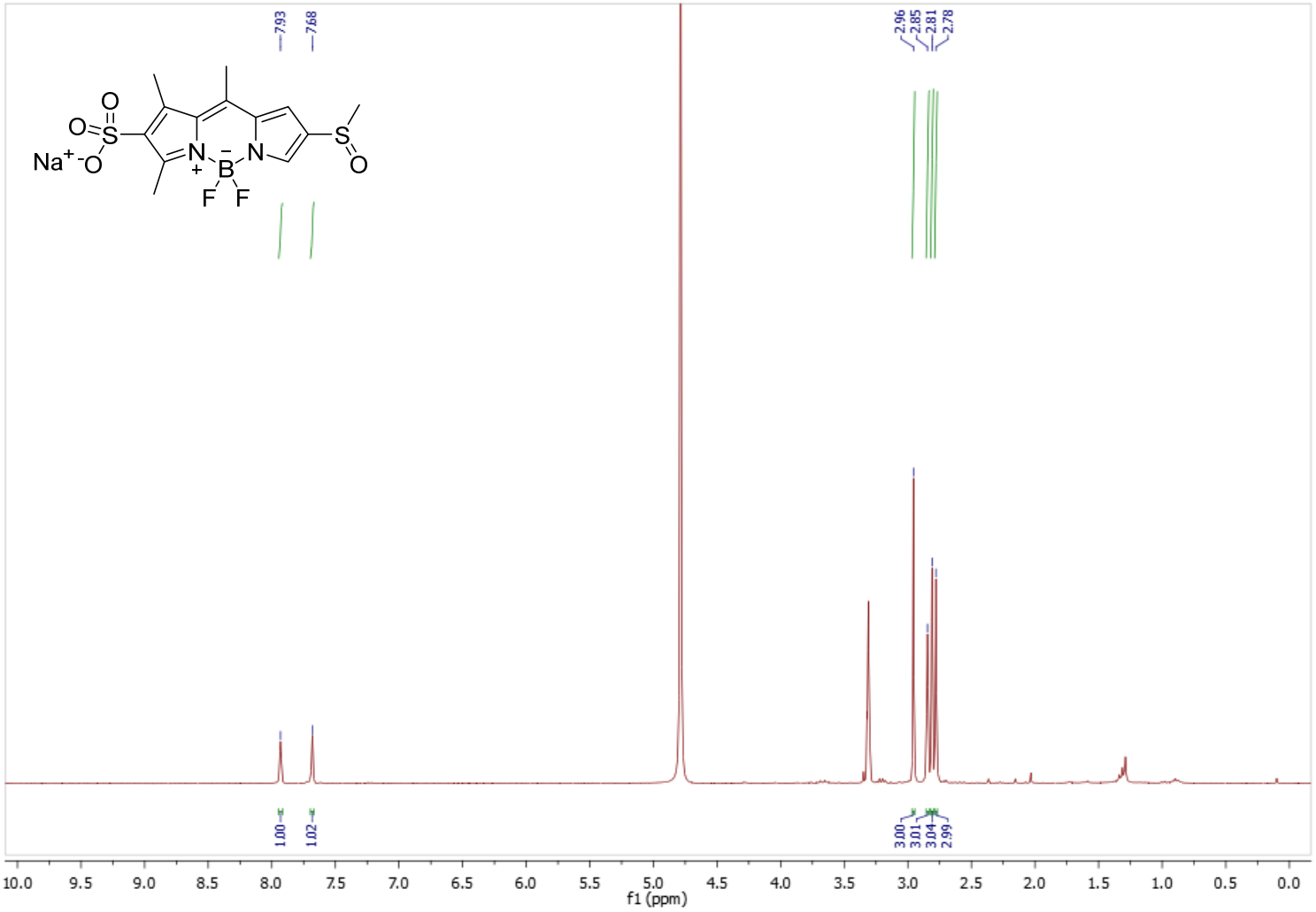

Figure S13. ^{1}H NMR of compound **1-(SOMe)(SO$_3$)** in CD$_3$OD.

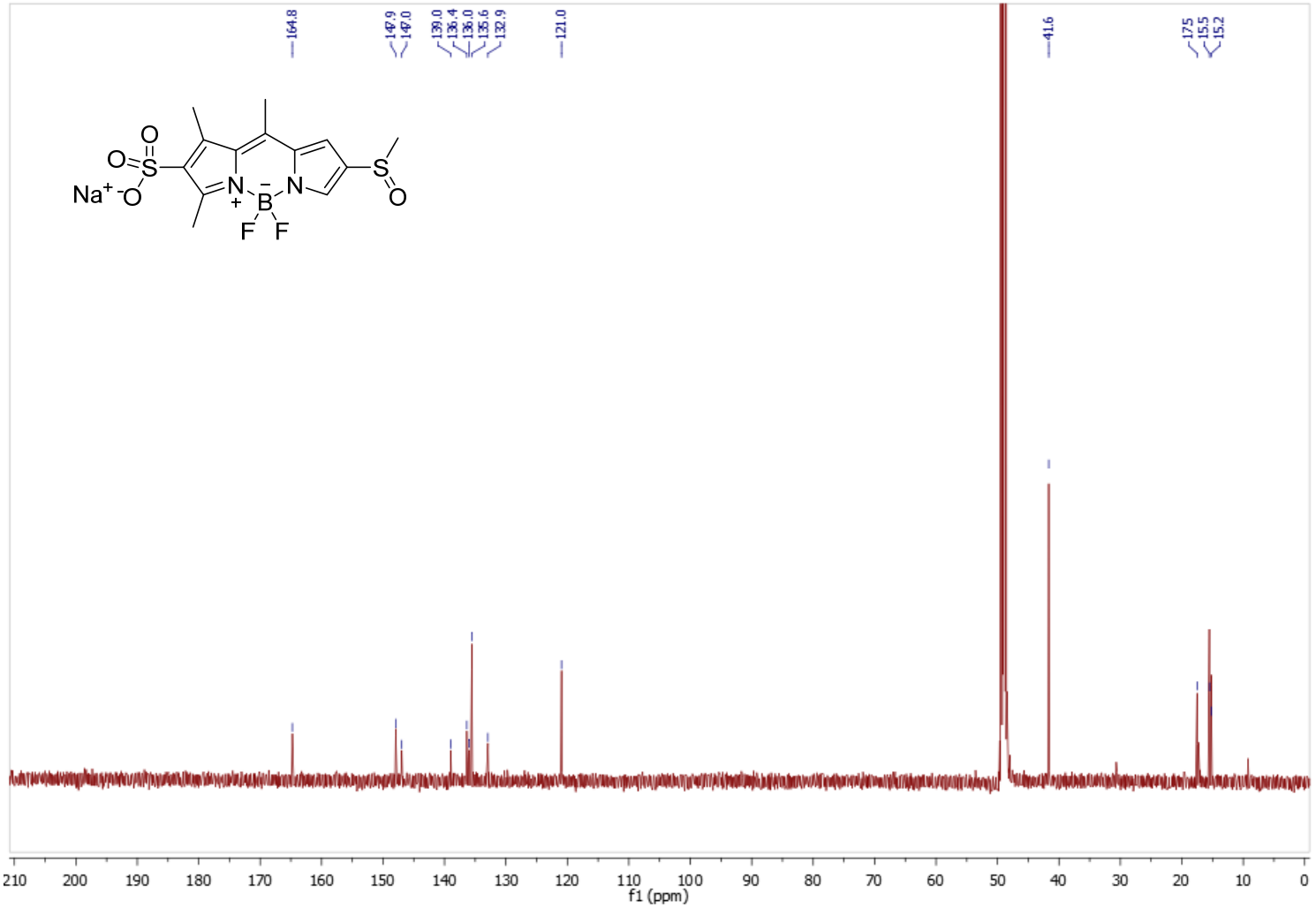

Figure S14 ^{13}C NMR of **1-(SOMe)(SO_3)** in CD_3OD.

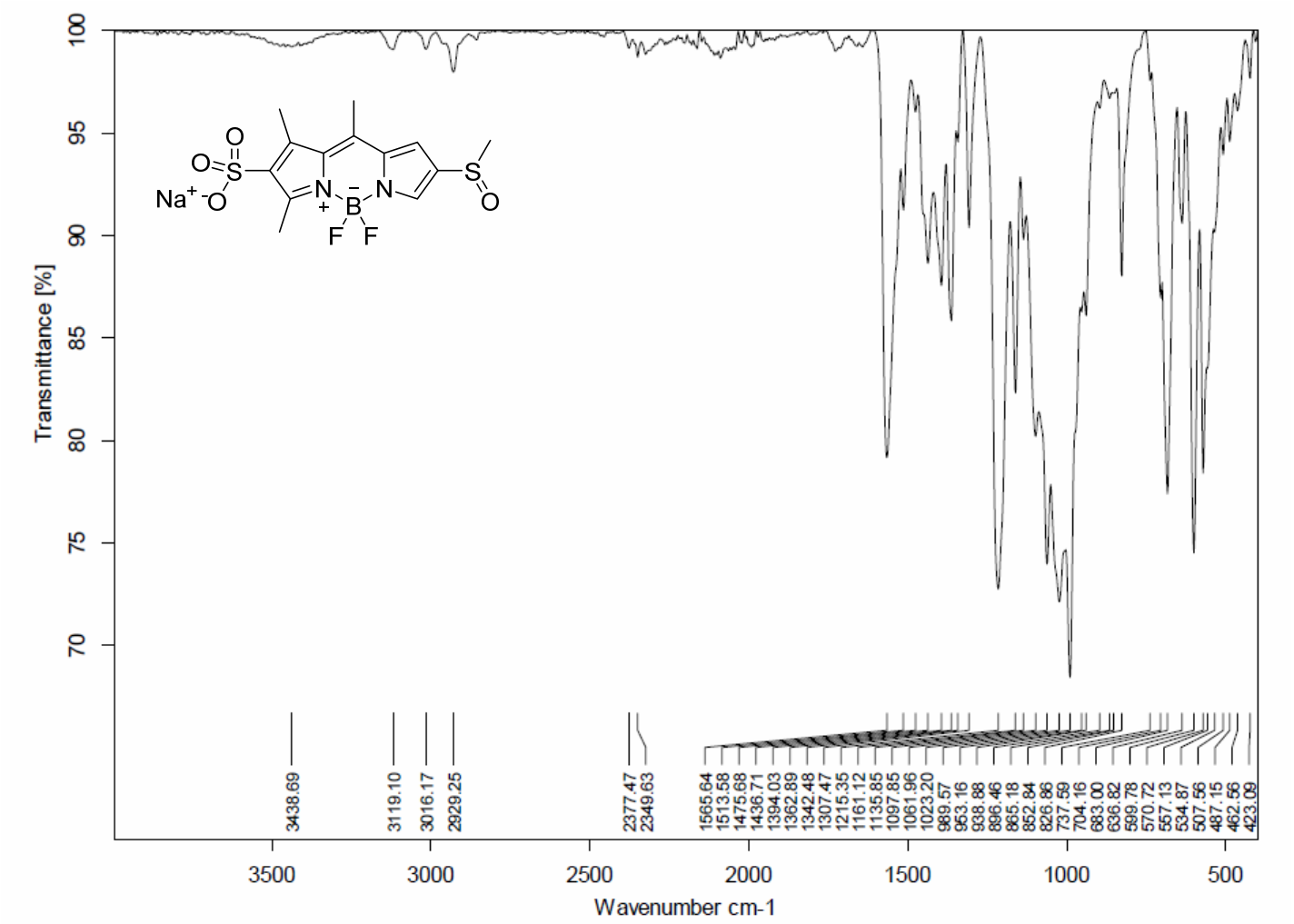

Figure S15. FTIR spectrum of **1-(SOMe)(SO_3)**.

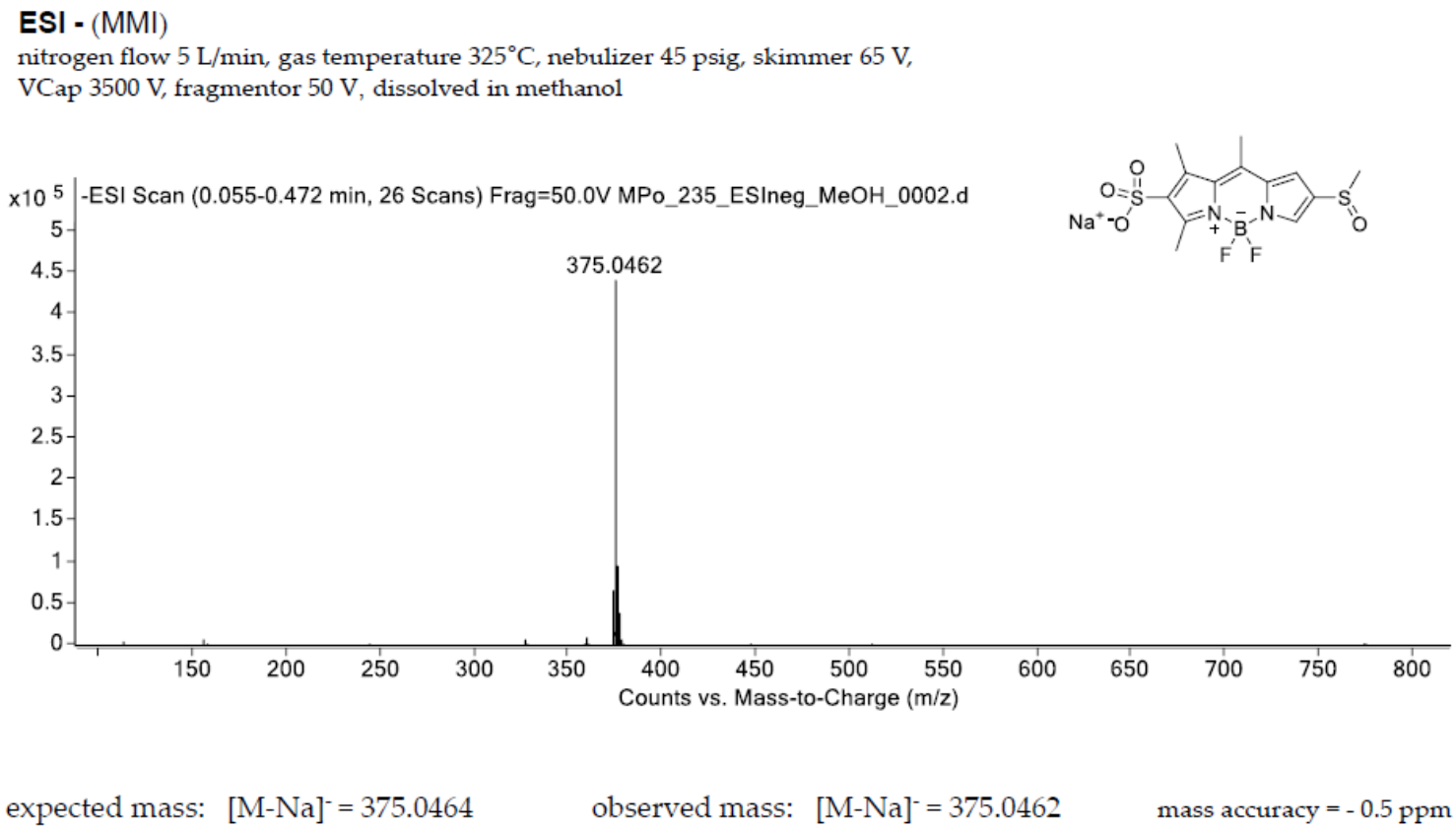

Figure S16. HRMS (ESI-) spectrum of **1-(SOMe)(SO_3)**.

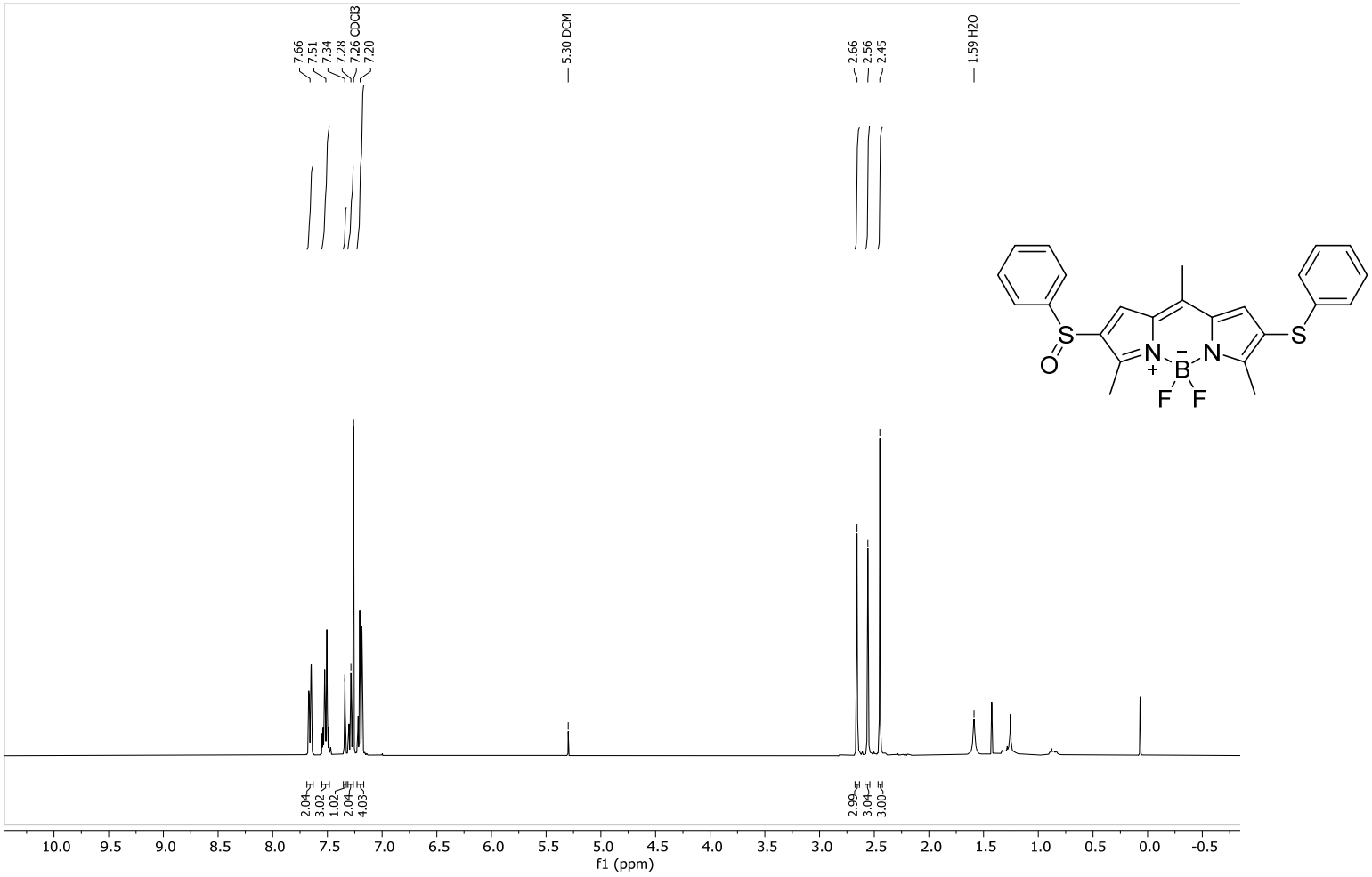

Figure S17. ^{1}H NMR of **2-(SOPh)(SPh)** in $CDCl_3$.

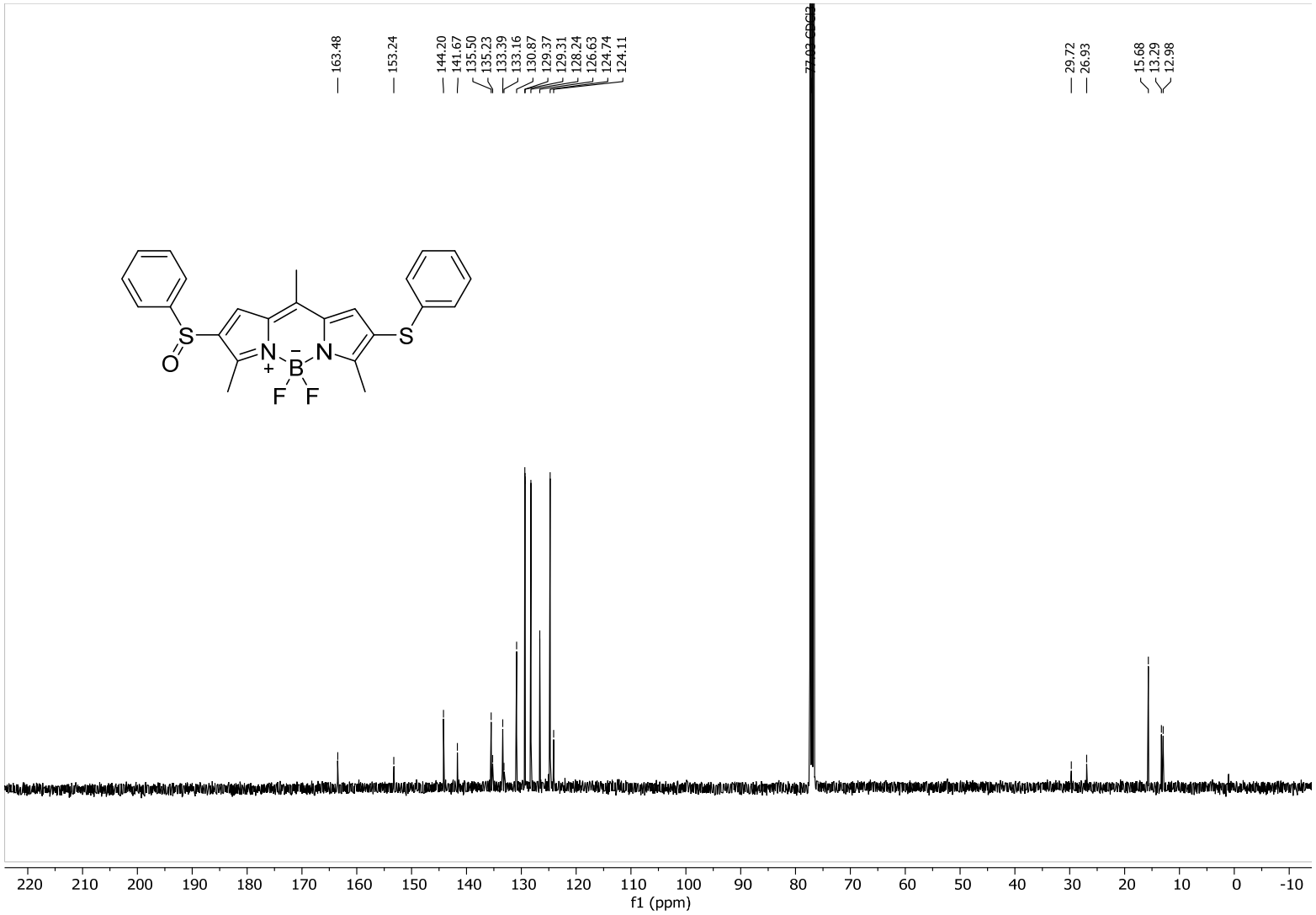

Figure S18. ^{13}C NMR of **2-(SOPh)(SPh)** in $CDCl_3$.

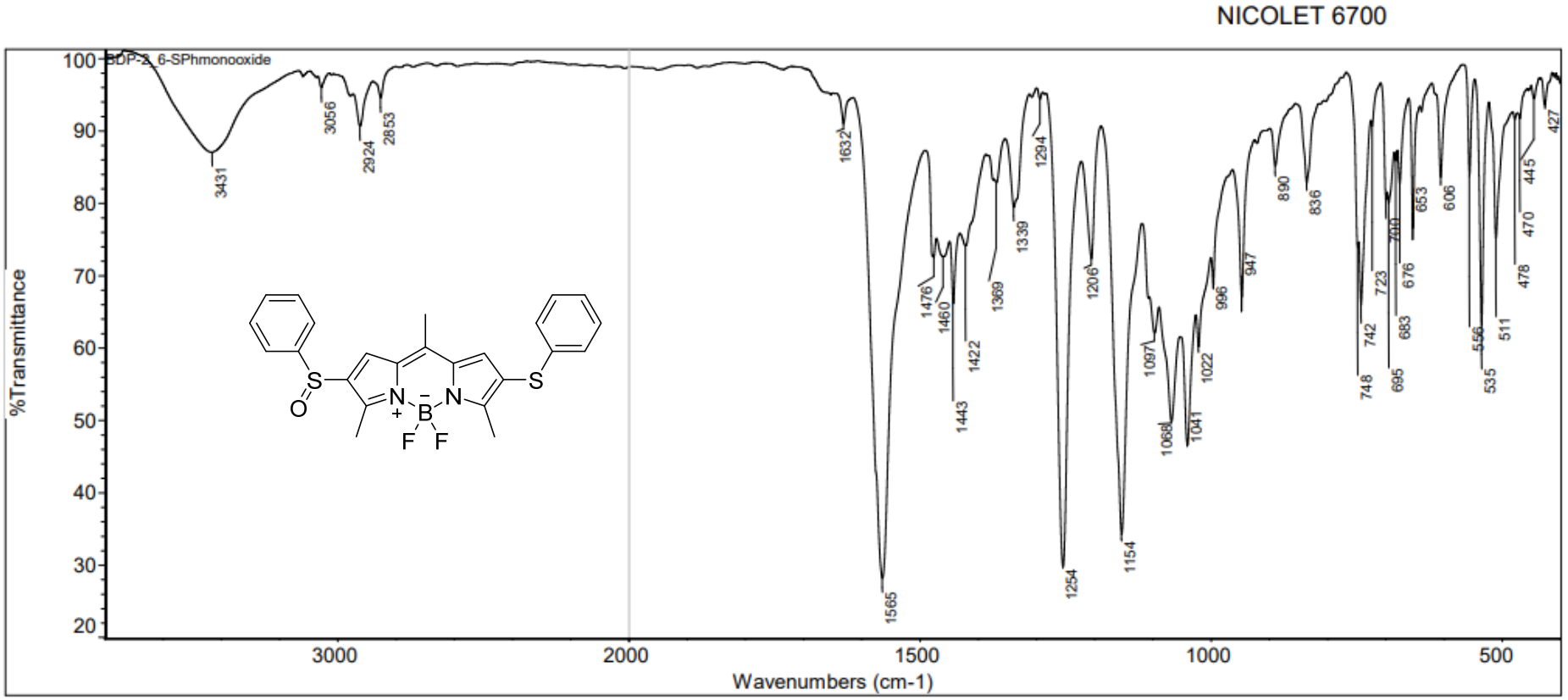

Figure S19. FTIR spectrum of **2-(SOPh)(SPh)**.

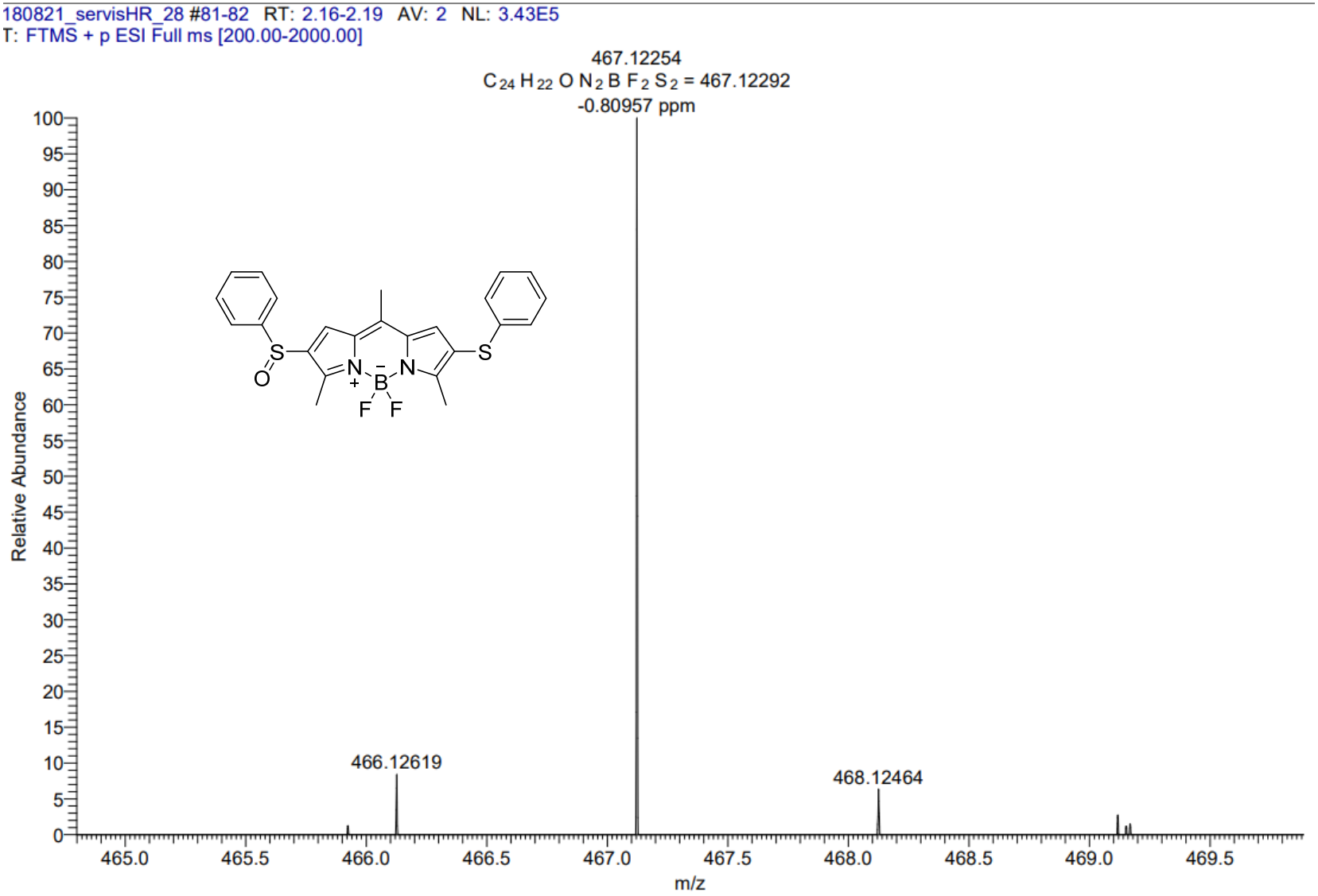

Figure S20. HRMS (ESI +) spectrum of **2-(SOPh)(SPh)**.

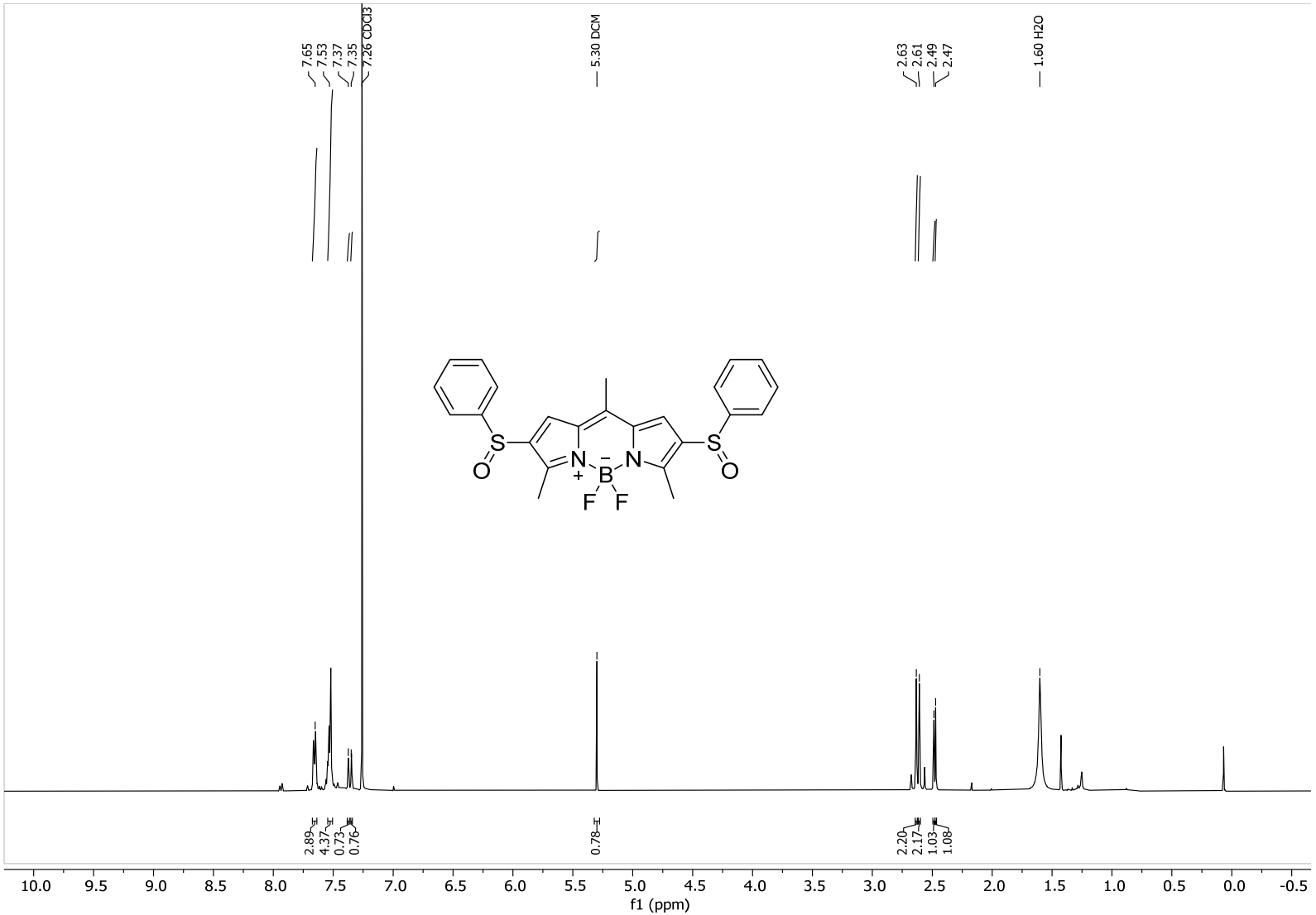

Figure S21. ^{1}H NMR of **2-(SOPh)(SOPh)** in $CDCl_3$.

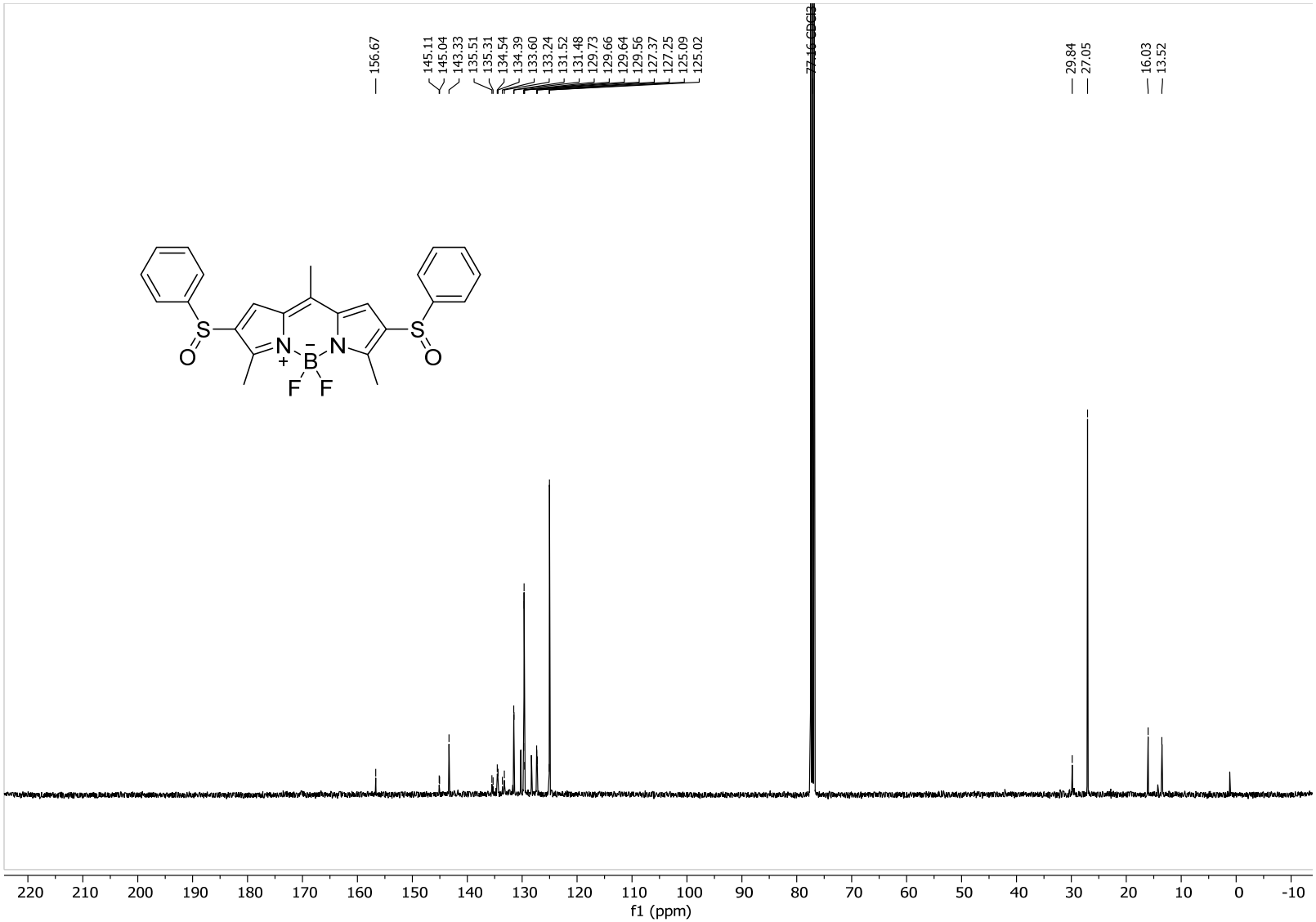

Figure S22. ^{13}C NMR of **2-(SOPh)(SOPh)** in $CDCl_3$.

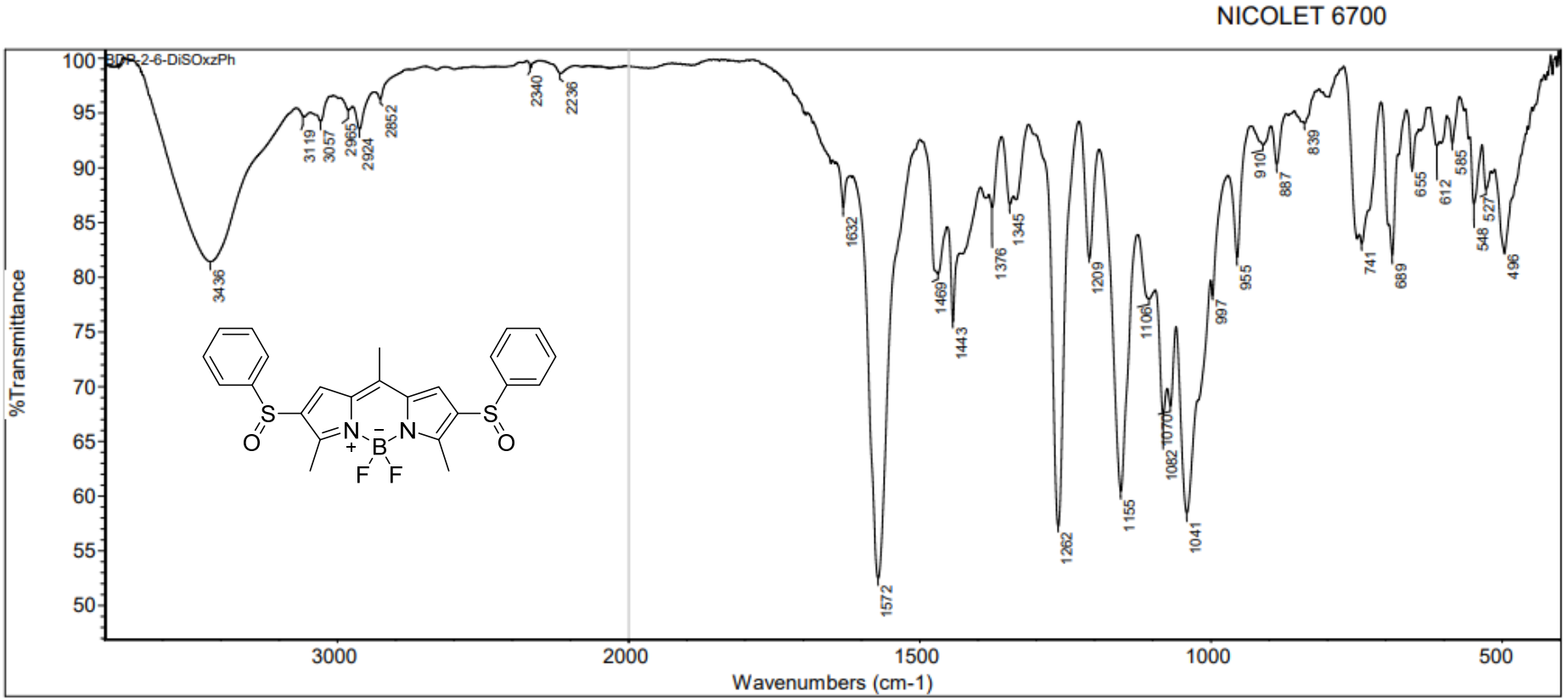

Figure S23. FTIR spectrum of **2-(SOPh)(SOPh)**.

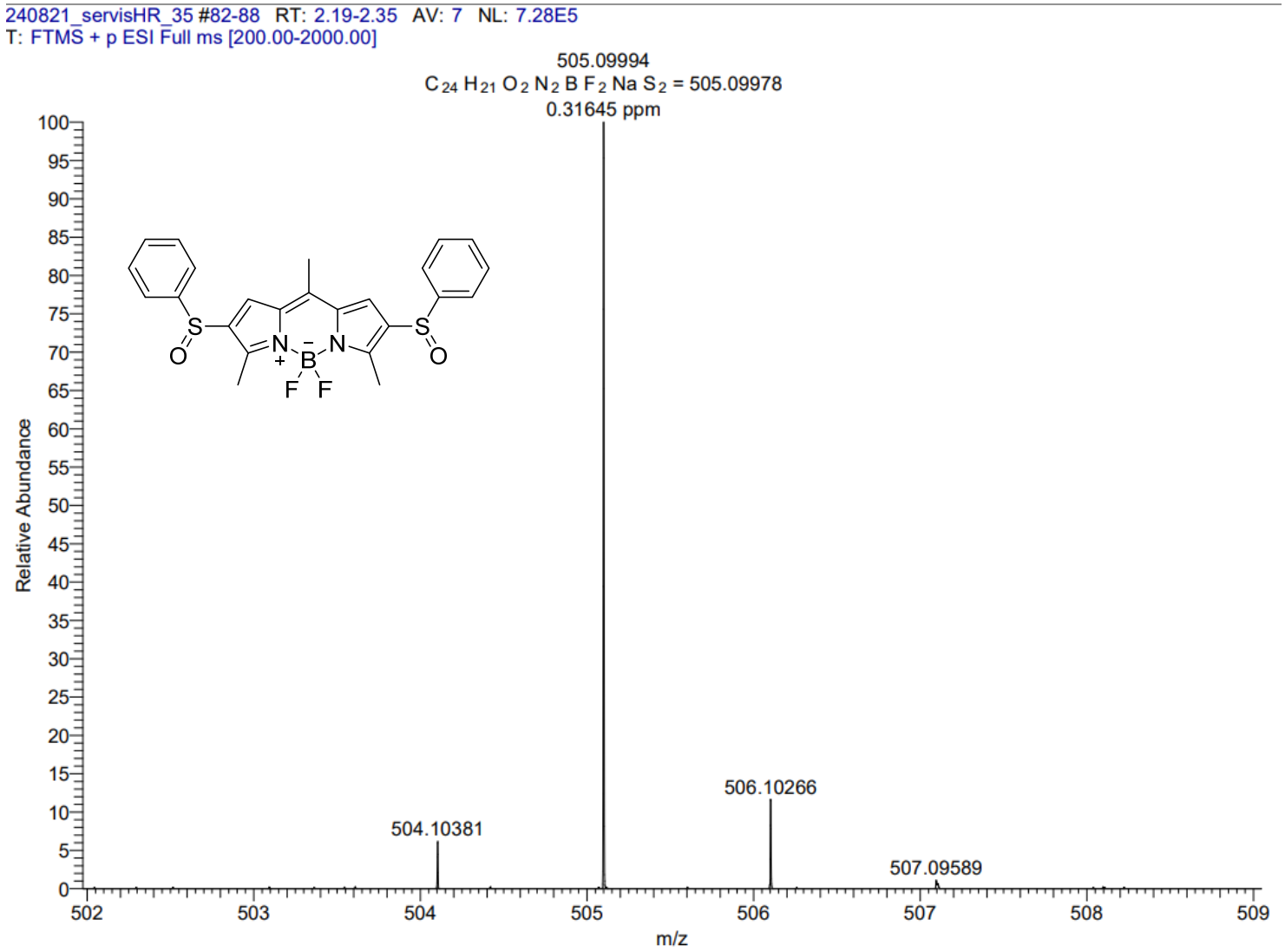

Figure S24. HRMS (ESI +) spectrum of **2-(SOPh)(SOPh)**.

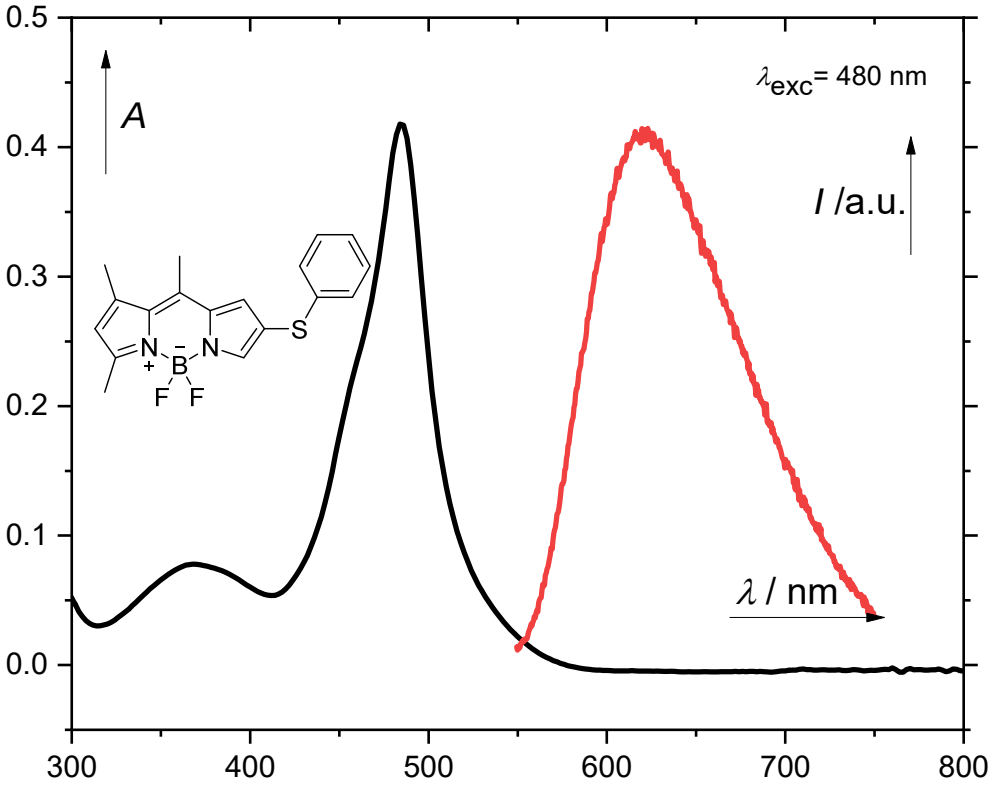

Figure S25. Absorption (black) and normalized emission (red, λ_{exc} = 480 nm) spectra of **1-SPh** in methanol.

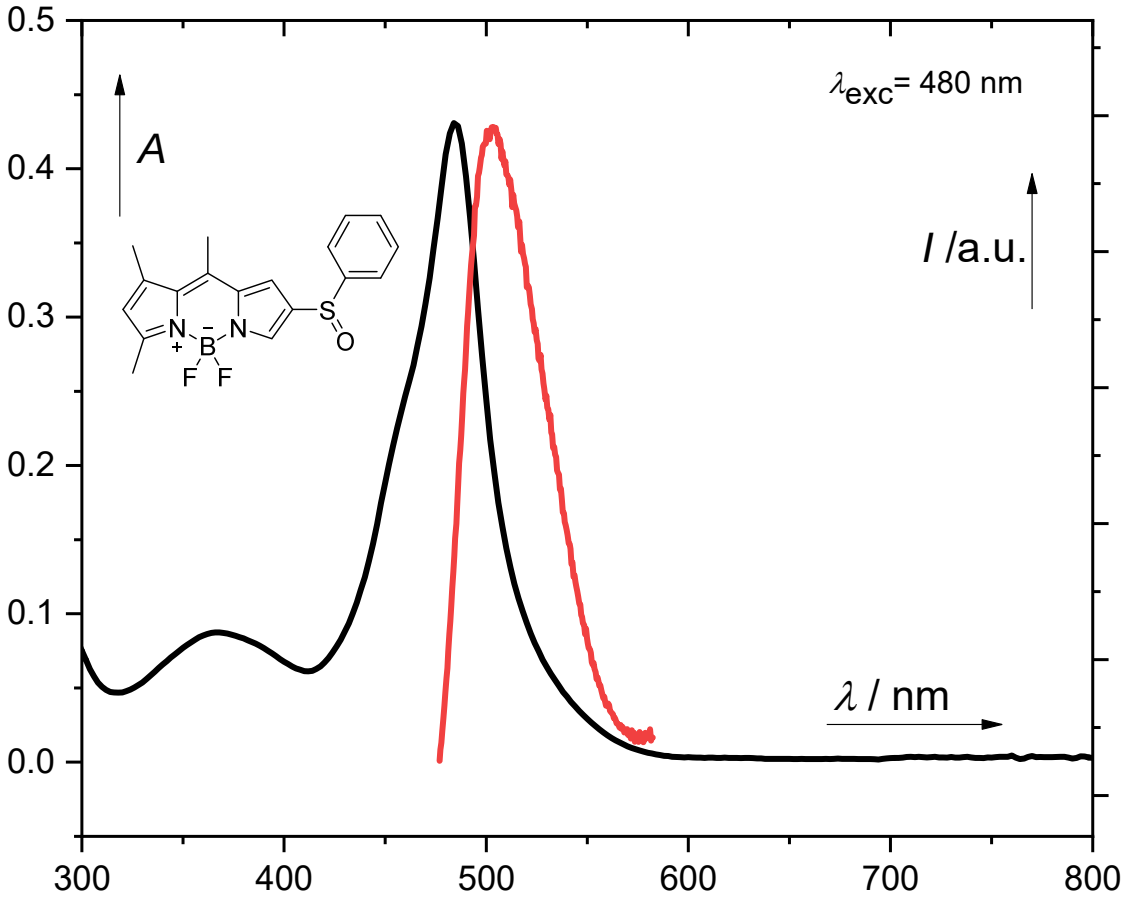

Figure S26. Absorption (black) and normalized emission (red, λ_{exc} = 480 nm) spectra of **1-SOPh** in methanol.

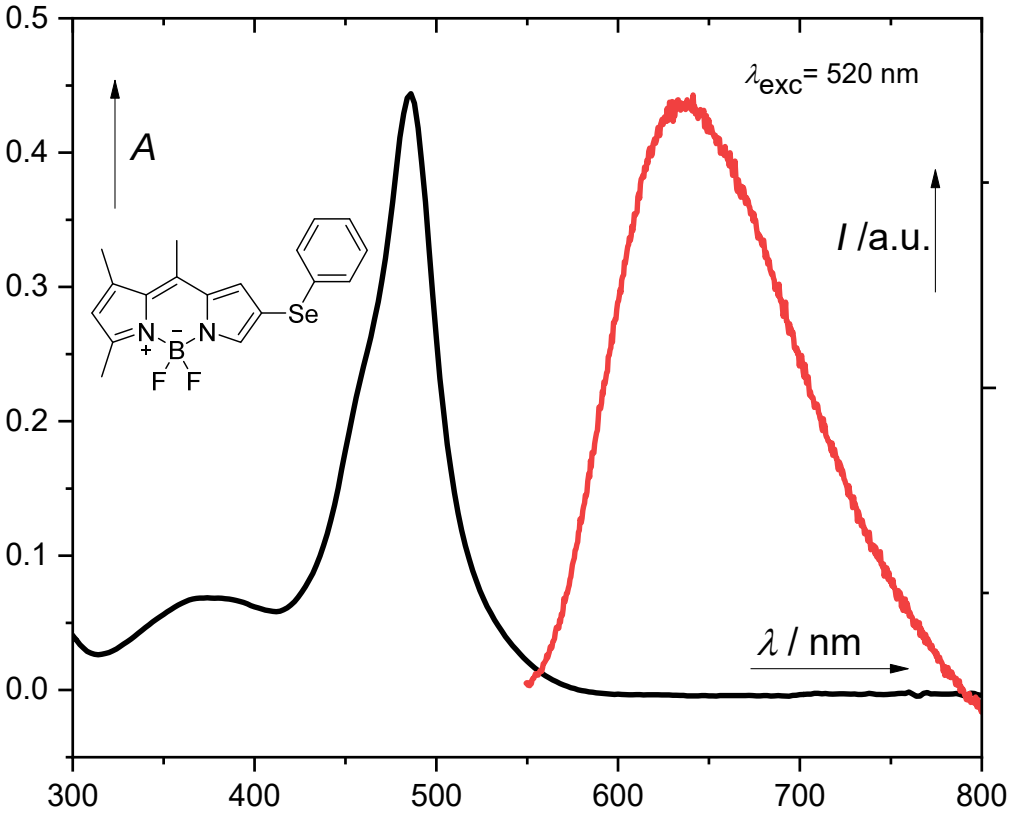

Figure S27. Absorption (black) and normalized emission (red, λ_{exc} = 520 nm) spectra of **1-SePh** in methanol.

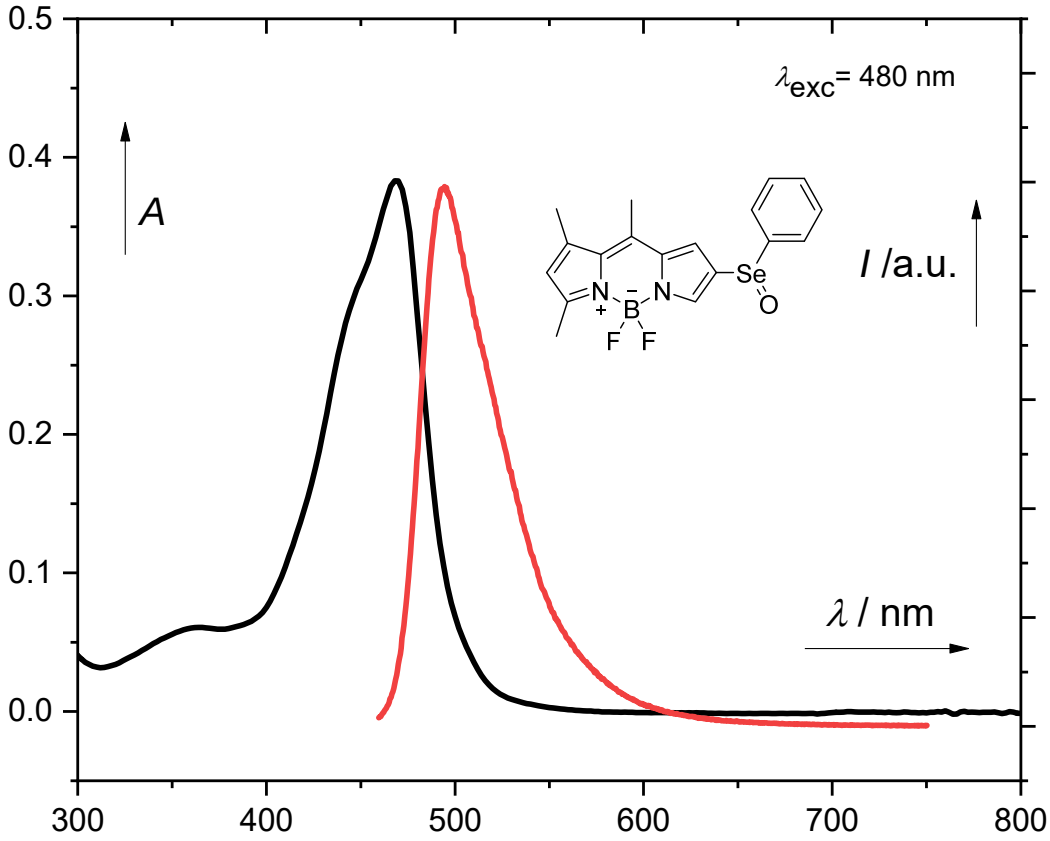

Figure S28. Absorption (black) and normalized emission (red, λ_{exc} = 480 nm) spectra of **1-SeOPh** in methanol.

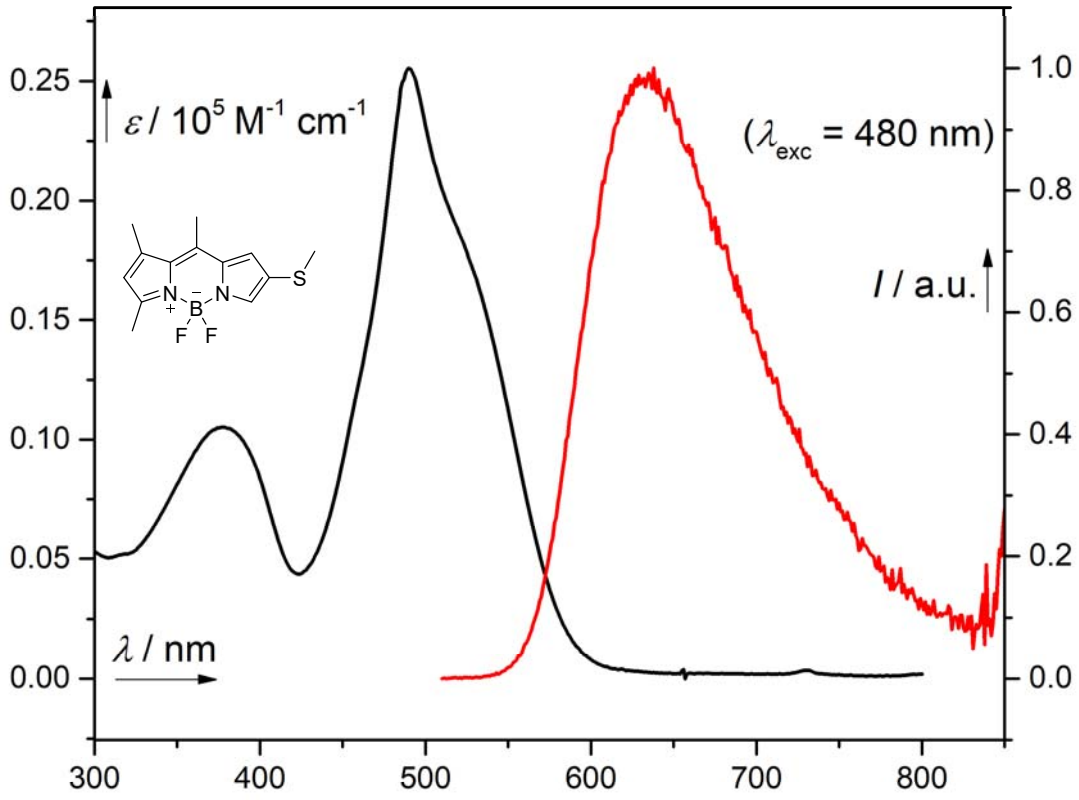

Figure S29. Absorption (black) and normalized emission (red, λ_{exc} = 480 nm) spectra of **1-SMe** in acetonitrile.

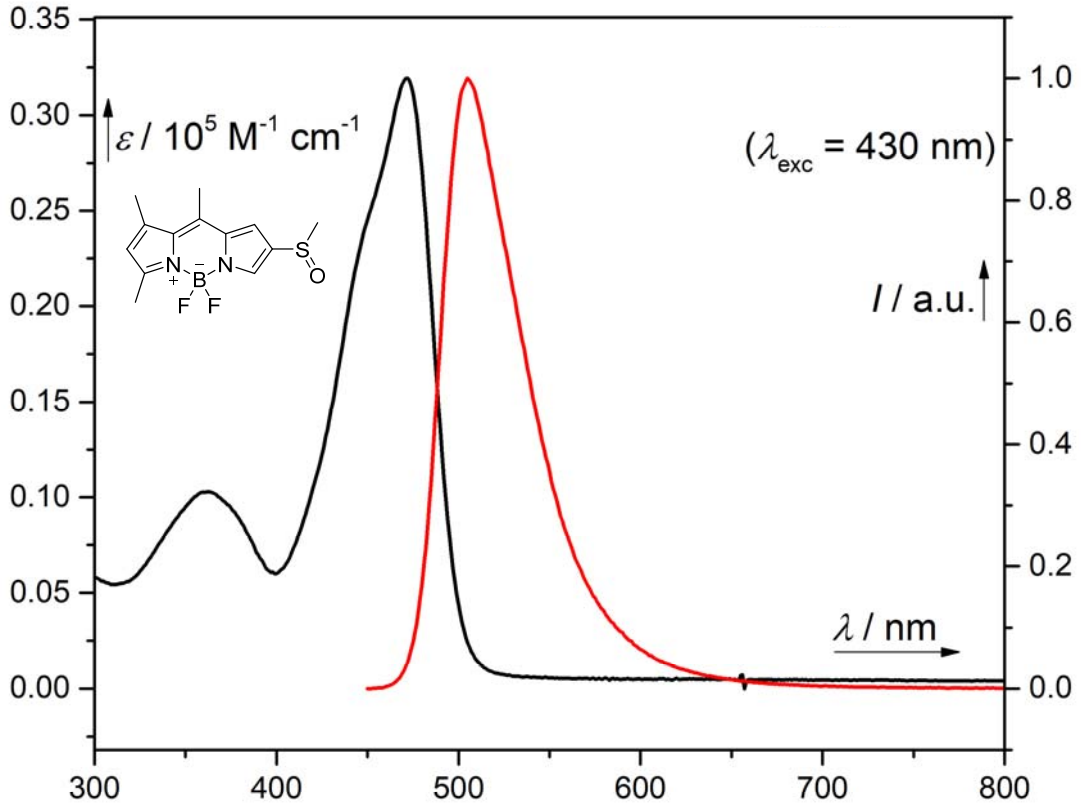

Figure S30. Absorption (black) and normalized emission (red, λ_{exc} = 430 nm) spectra of **1-SOMe** in acetonitrile.

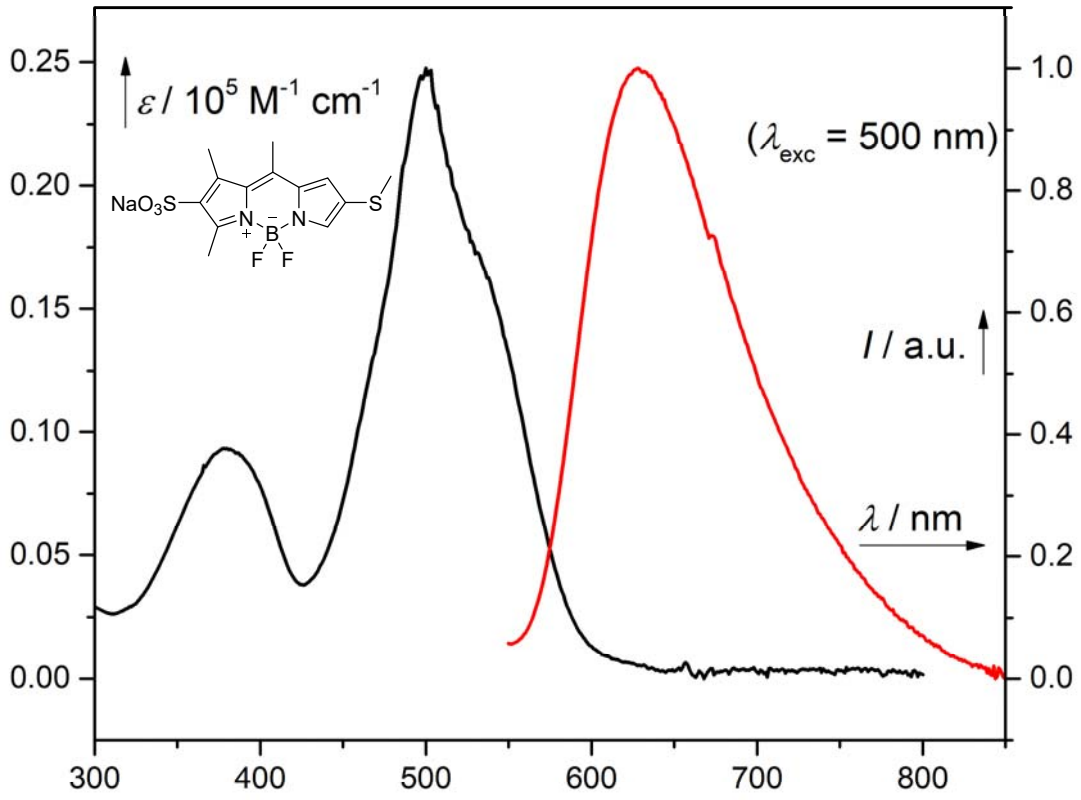

Figure S31. Absorption (black) and normalized emission (red, λ_{exc} = 500 nm) spectra of **1-(SMe)(SO$_3$)** in acetonitrile.

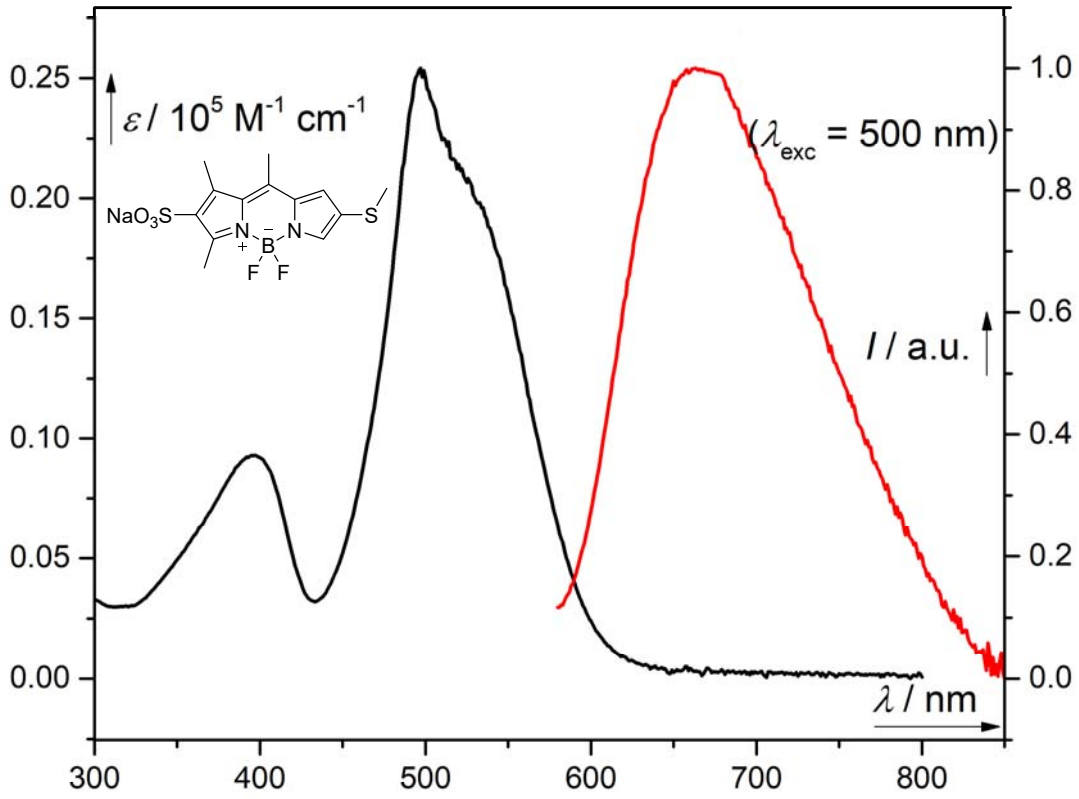

Figure S32. Absorption (black) and normalized emission (red, λ_{exc} = 500 nm) spectra of **1-(SMe)(SO$_3$)** in PBS (pH = 7.4).

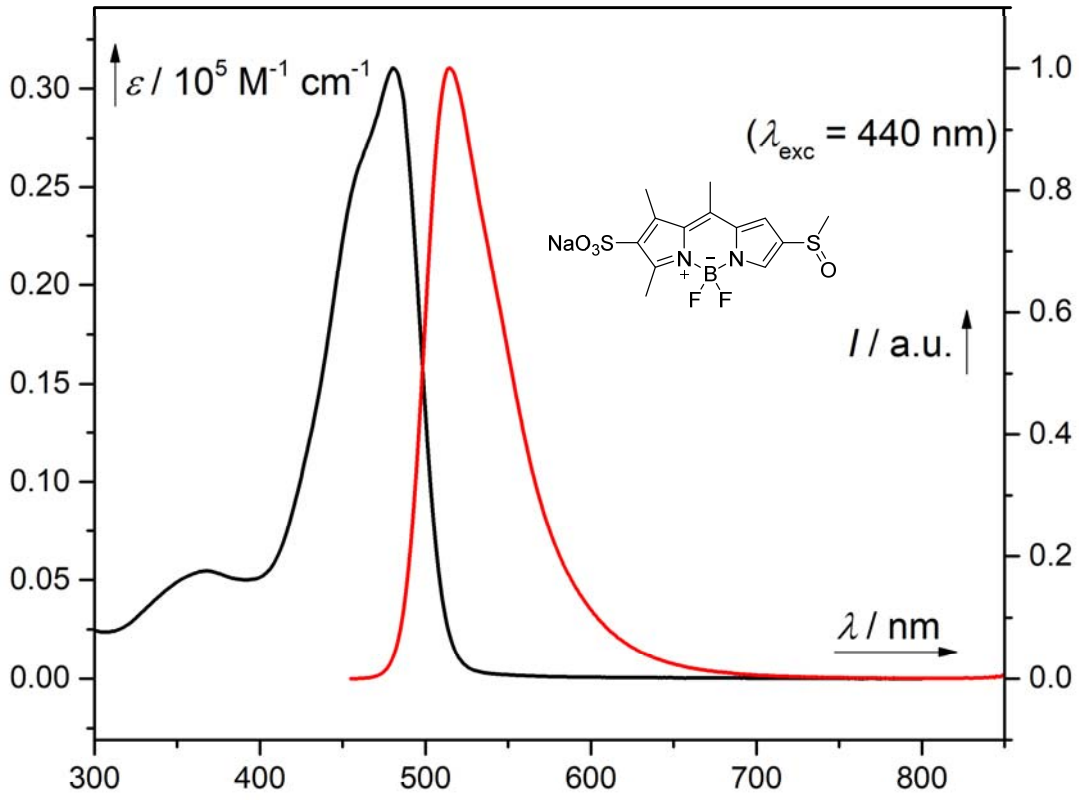

Figure S33. Absorption (black) and normalized emission (red, λ_{exc} = 440 nm) spectra of **1-(SOMe)(SO_3)** in acetonitrile.

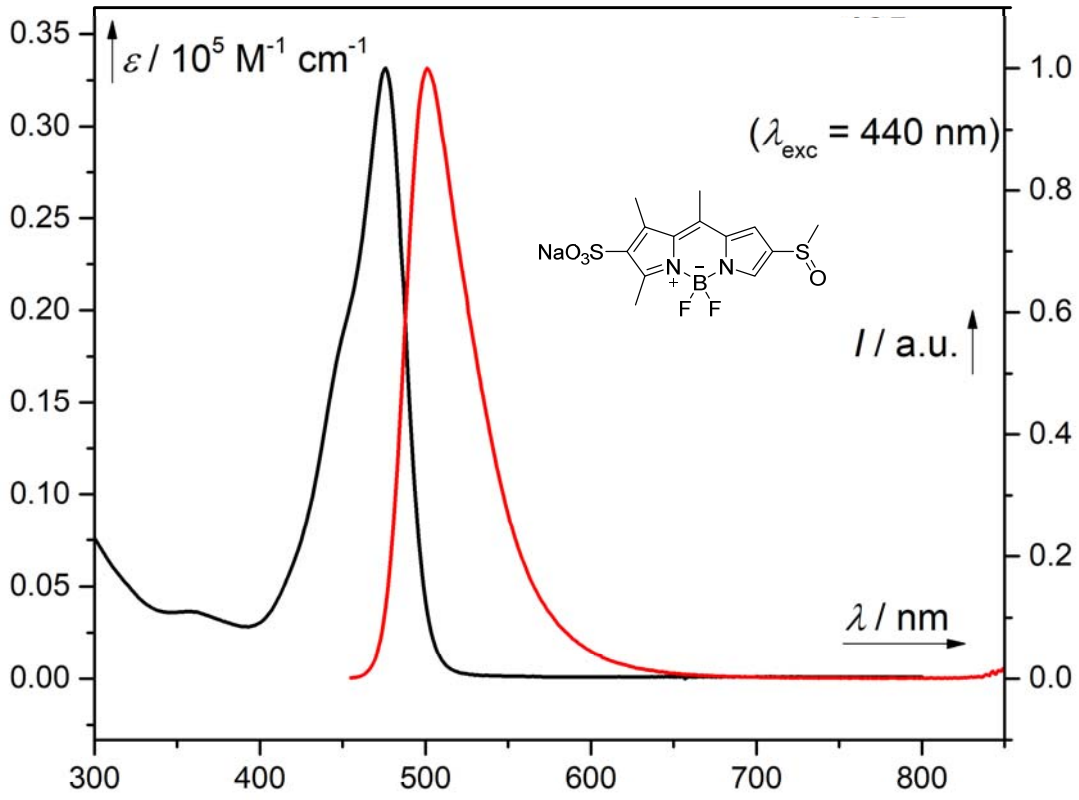

Figure S34. Absorption (black) and normalized emission (red, λ_{exc} = 440 nm) spectra of **1-(SOMe)(SO_3)** in PBS (pH = 7.4).

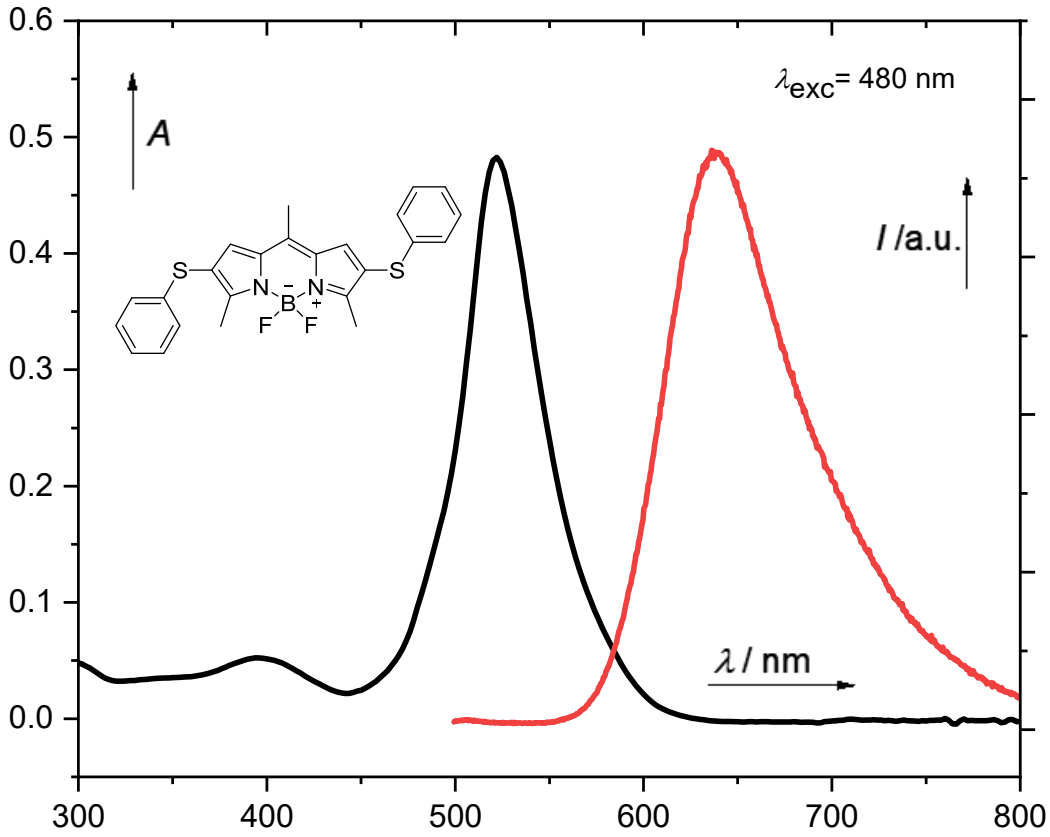

Figure S35. Absorption (black) and normalized emission (red, λ_{exc} = 480 nm) spectra of **2-(SPh)(SPh)** in methanol.

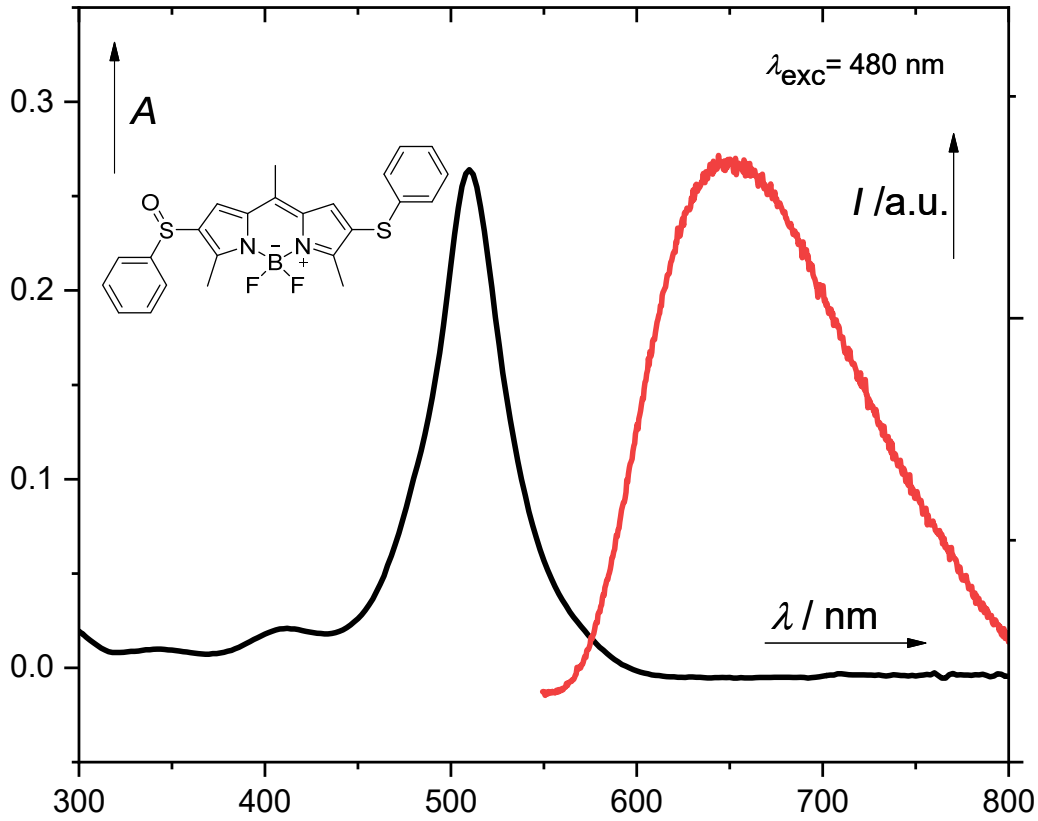

Figure S36. Absorption (black) and normalized emission (red, λ_{exc} = 480 nm) spectra of **2-(SOPh)(SPh)** in methanol.

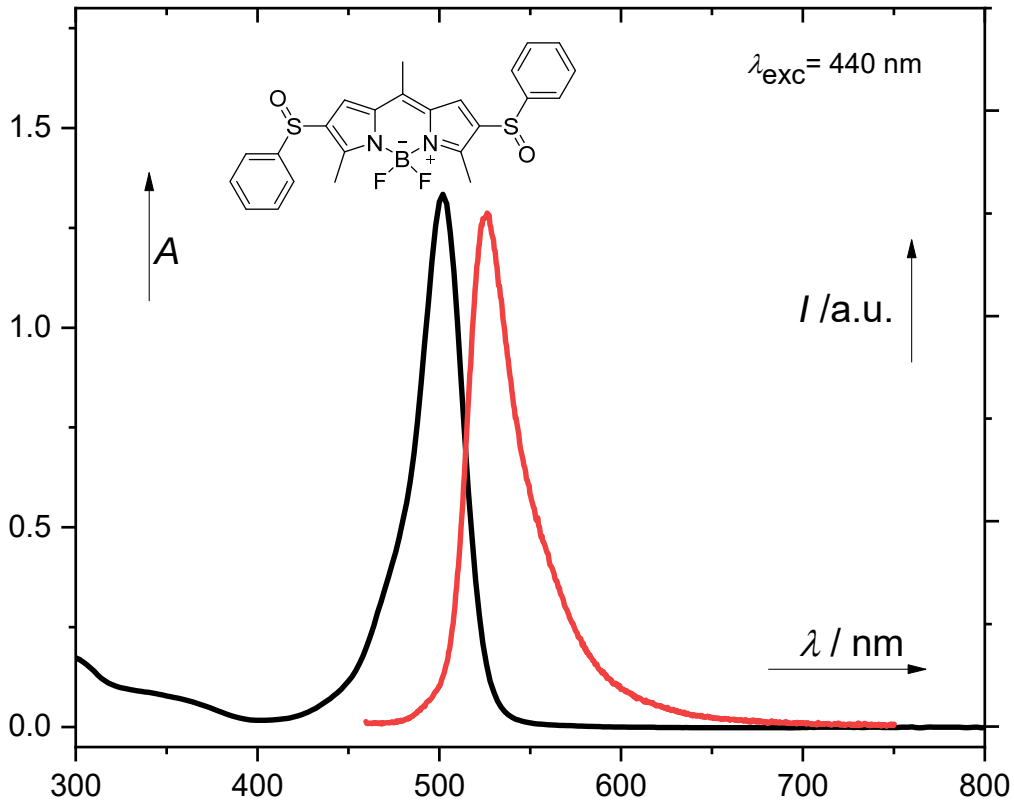

Figure S37. Absorption (black) and normalized emission (red, λ_{exc} = 440 nm) spectra **2-(SOPh)(SOPh)** in methanol.

Enzymatic Experiments

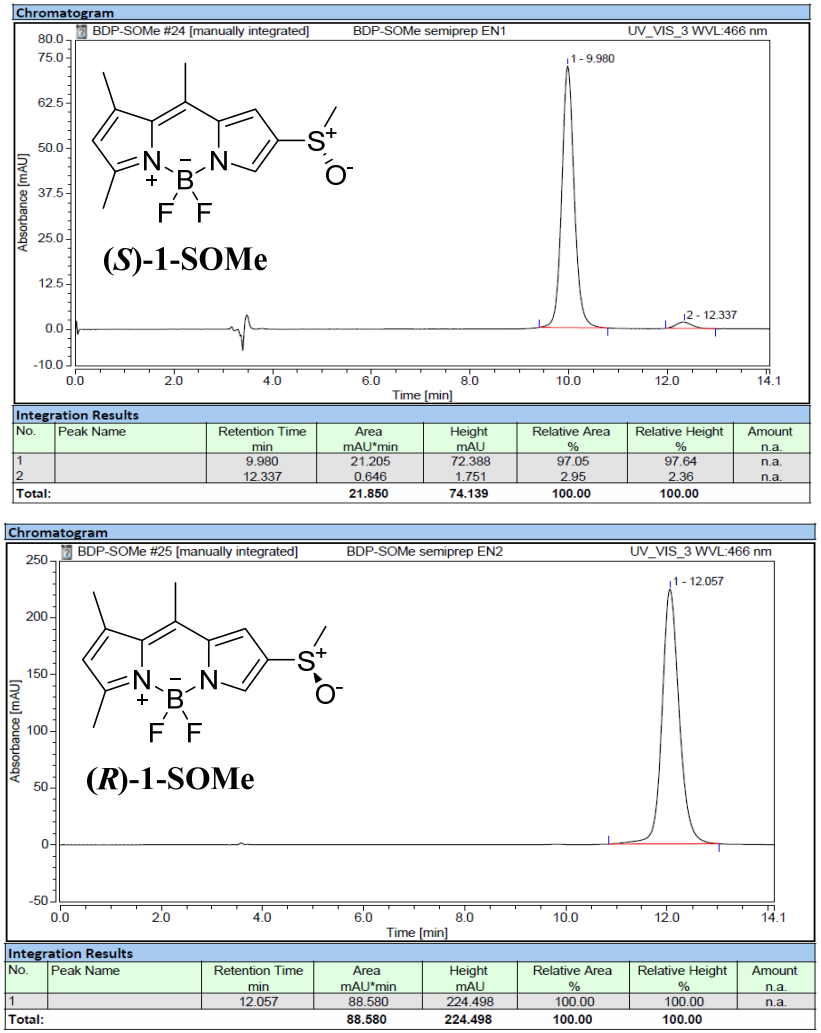

Figure S38. Chromatograms of **(*S*)-1-SOMe** (top) and **(*R*)-1-SOMe** (bottom) separated by chiral HPLC (retention times given in min).

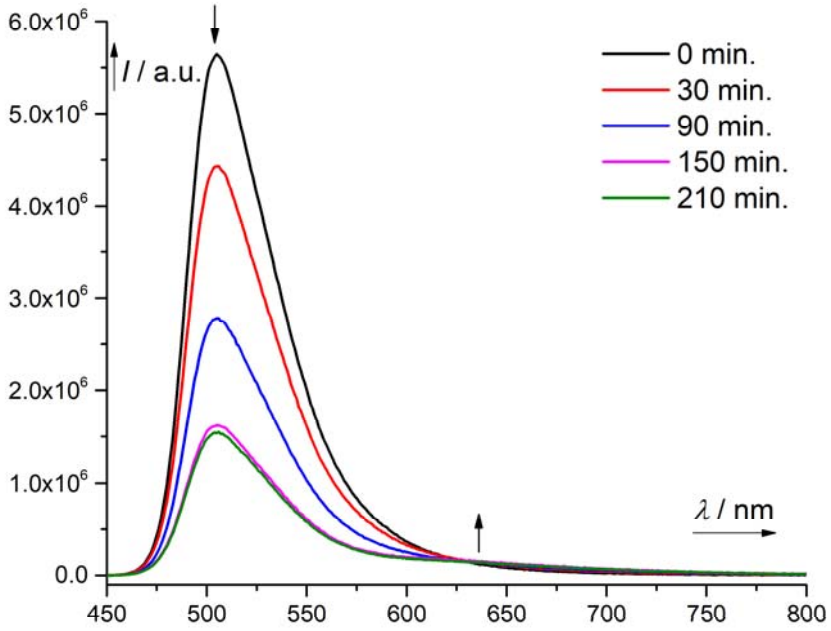

Figure S39. Decrease in fluorescence of **(*S*)-1-SOMe** in the presence of MsrA (λ_{exc} = 430 nm).

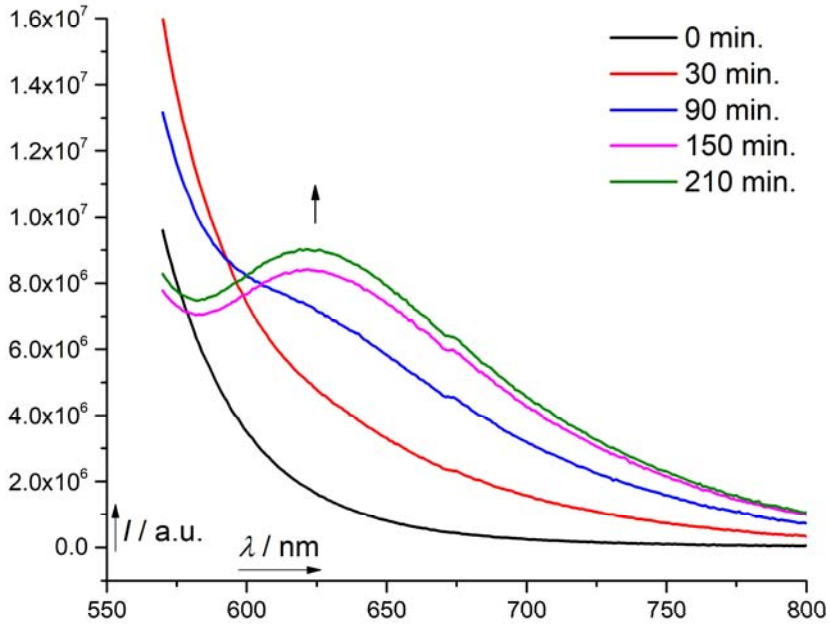

Figure S40. Increase in fluorescence of **1-SMe** in the presence of MsrA (λ_{exc} = 480 nm).

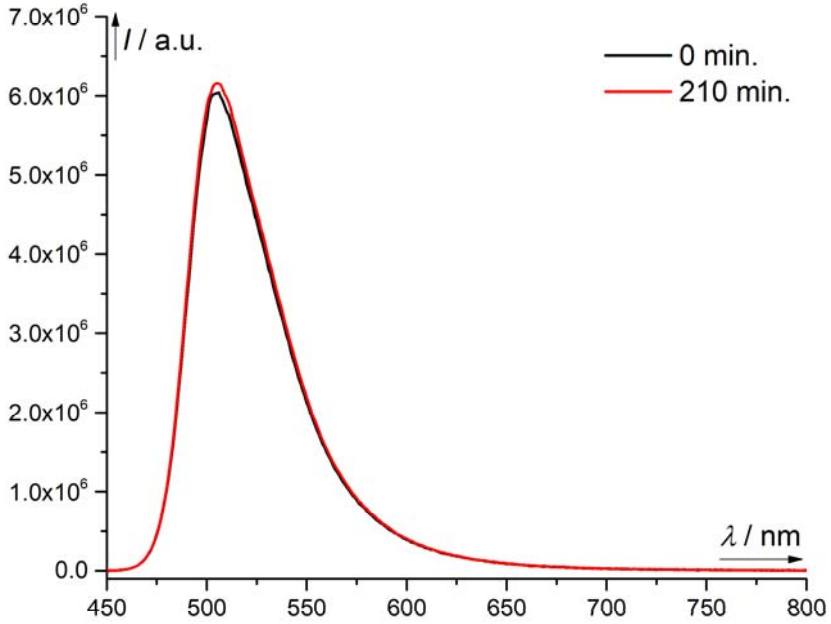

Figure S41. No change in fluorescence of **(*R*)-1-SOMe** in the presence of MsrA (λ_{exc} = 430 nm).

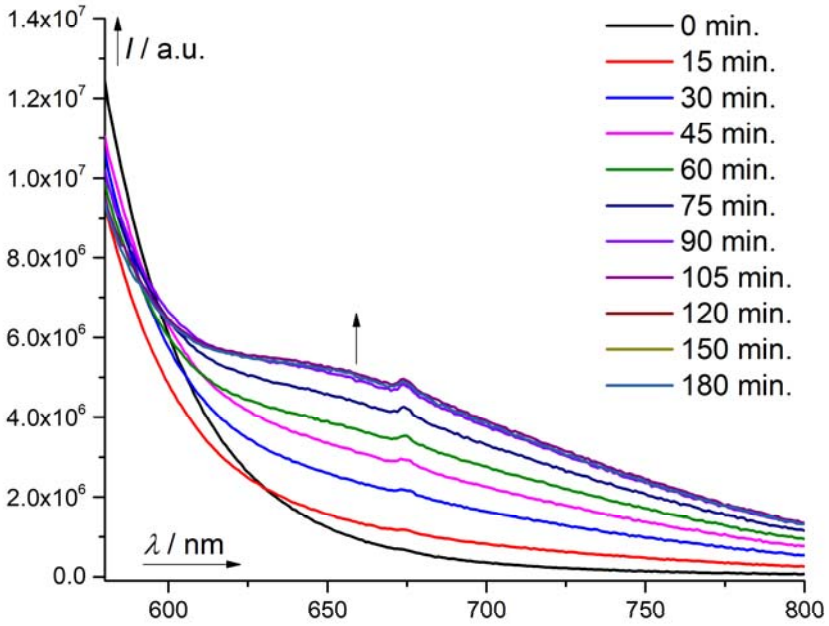

Figure S42. Increase in fluorescence of **1-(SMe)(SO_3)** in the presence of MsrA (λ_{exc} = 500 nm).

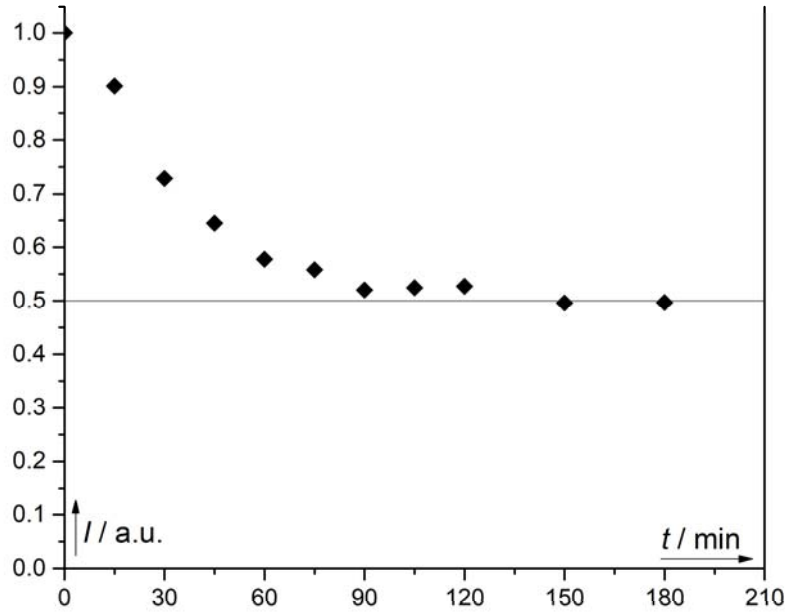

Figure S43. Decrease of fluorescence of ***rac*-1-(SOMe)(SO_3)** at λ_{em} = 501 nm within 200 min.

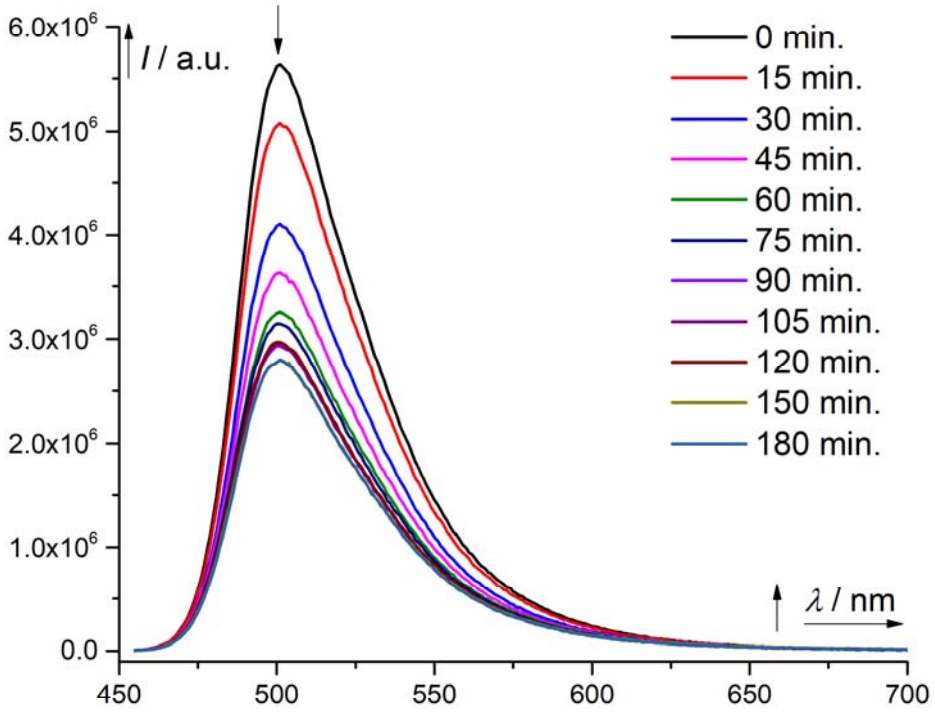

Figure S44. Decrease in fluorescence of ***rac*-1-(SOMe)(SO_3)** in the presence of MsrA (λ_{exc} = 440 nm).

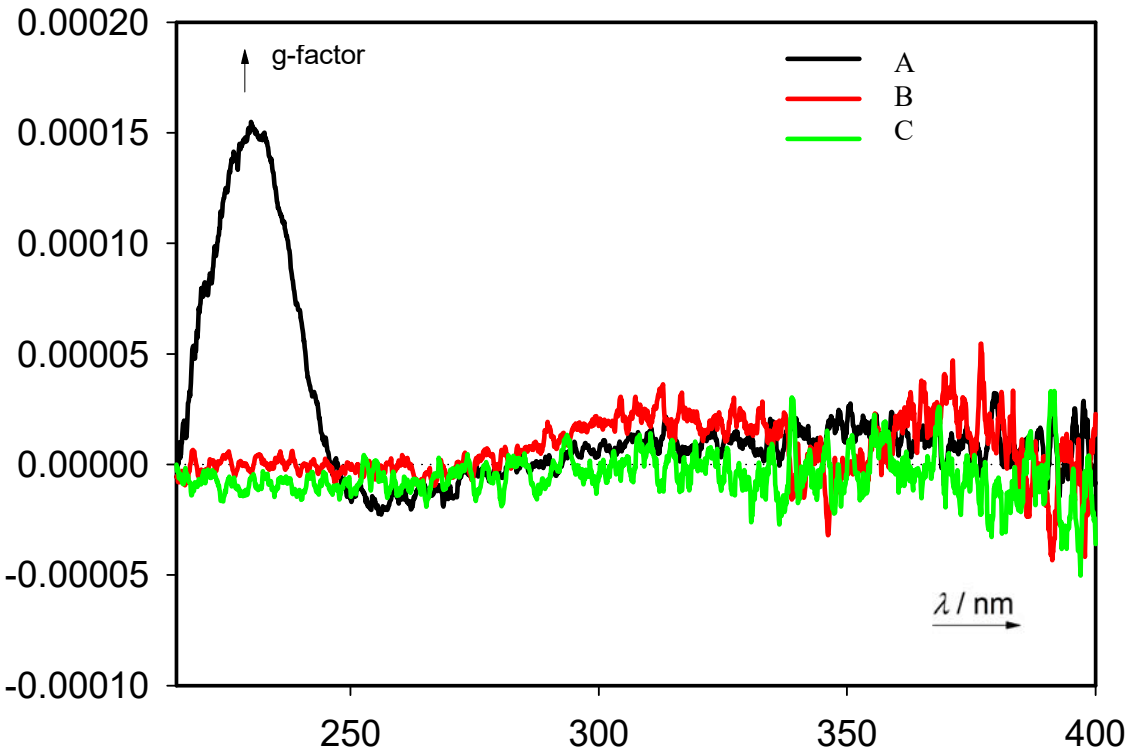

Figure S45. Circular dichroism spectra of (A, black) ***rac*-1-(SOMe)(SO_3)** after the enzymatic reaction was completed, i.e., the (*S*)-enantiomer was converted to **1-(SMe)(SO_3)**, (B, red) ***rac*-1-(SOMe)(SO_3)** in the enzymatic buffer (a control reaction without MsrA), (C, green) ***rac*-1-(SOMe)(SO_3)** in PBS.

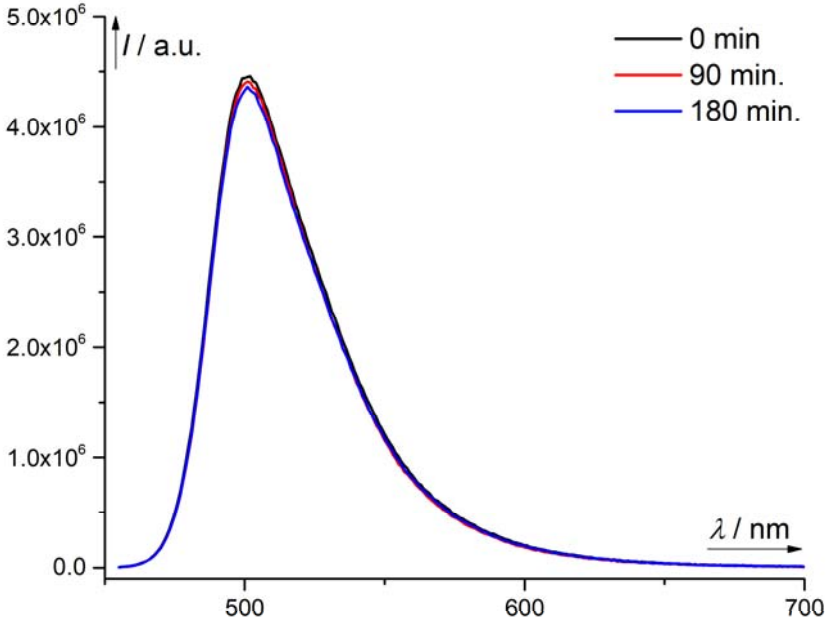

Figure S46. Control experiment of ***rac*-1-(SOMe)(SO_3)** without MsrA (λ_{exc} = 440 nm).

Redox Sensing

Redox Cycles. The redox cycles were monitored by a fluorescence response of the oxidized (**1-SeOPh**) and reduced (**1-SePh**) forms. **1-SePh** in a dichloromethane/methanol (1/9, v/v, 2 mL, c = 10 μM) solution was oxidized to **1-SeOPh** by NaOCl (5 – 9 eq., maximum increase of the fluorescence intensity). The mixture was stirred for 1 min before the addition of excess H_2S caused the quantitative reduction to **1-SePh** (a maximum decrease of the fluorescence intensity after addition of H_2S). H_2S was generated from the reaction of the corresponding amount of Na_2S (5 eq.) with HCl; the produced gas was transferred to a cuvette via cannula in a flow of N_2. The redox cycles were repeated 5 times. All spectra were measured with λ_{ex} = 460 nm and λ_{em} = 496 nm. The numbers in the diagram shown in Figure 3c in the main text represent the following conditions: **0**: starting **1-SePh**, **0.5**: +5 eq. NaClO, **1**: +5 eq. H_2S, **1.5**: +9 eq. NaClO, **2**: +5 eq. H_2S, **2.5**: +9 eq. NaClO, **3**: +5 eq. H_2S, **3.5**: + 9 eq. NaClO, **4**: +5 eq. H_2S, **4.5**: +9 eq. NaClO, **5**: +5 eq. H_2S. The redox cycles were not measured for a **1-SPh**/**1-SOPh** system because a quantitative reduction of **1-SOxyPh** by H_2S was not possible.

Sensitivity to ROS. The sensitivity to ROS was monitored by the fluorescence response of the oxidized forms (**1-SOPh** or **1-SeOPh**). A substrate, **1-SPh** (c = 8 μM) or **1-SePh** (c = 20 μM), was treated with 10 equivalents of ROS (NaOCl, *m*-CPBA, $^1O_2$, H_2O_2 and OH•). The fluorescence response was measured after 20 min of stirring. The concentration of NaClO was determined from the absorption spectrum ($\varepsilon(292)$ = 350 M^{-1} cm^{-1}).

1-SePh (c = 10 μM) was also found to be sensitive to oxidation with endoperoxide products of a singlet oxygen-induced oxidation of 1,3-diphenylisobenzofuran (c = 50 μM) in the presence of methylene blue (c = 10 μM) in acetonitrile.

Sensitivity to Reducing Agents. 1-SOPh and **1-SeOPh** (c = 8 μM) were treated with 1 eq of areducing agent (L-ascorbic acid (L-AA), $NaHSO_3$, GSH, L-Cys, H_2S). The progress of the reduction was measured as the decrease of the fluorescence intensity.

Limit of Detection

The limit of detection of derivatives **1-SPh**, **1-SePh**, **1-SOPh**, and **1-SeOPh** was determined by gradual dilution of their solutions in methanol until the signal intensity was only ~5 times

higher than the background noise. An example of a dilution plot of **1-SOPh** in methanol is shown in Figure S47.

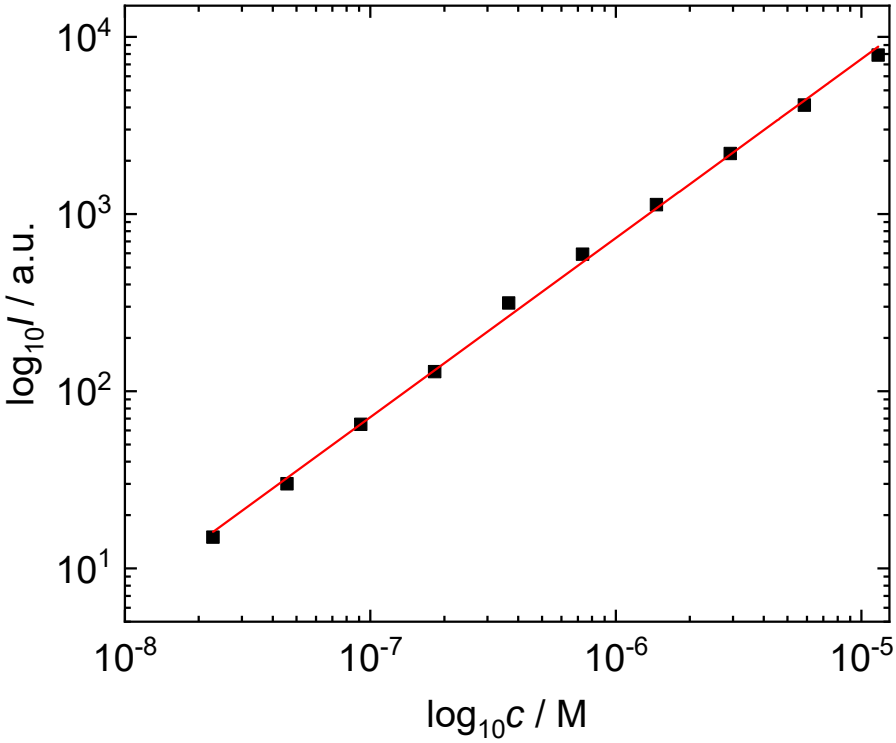

Figure S47. Dilution plot of **1-SOPh** in methanol.

Following limits of detection were found: **1-SPh** (2.2 ± 0.4 nM), **1-SePh** (20 ± 4 nM), **1-SOPh** (0.28 ± 0.06 nM), **1-SeOPh** (2.0 ± 0.4 nM). The results are visualized in Figure S48.

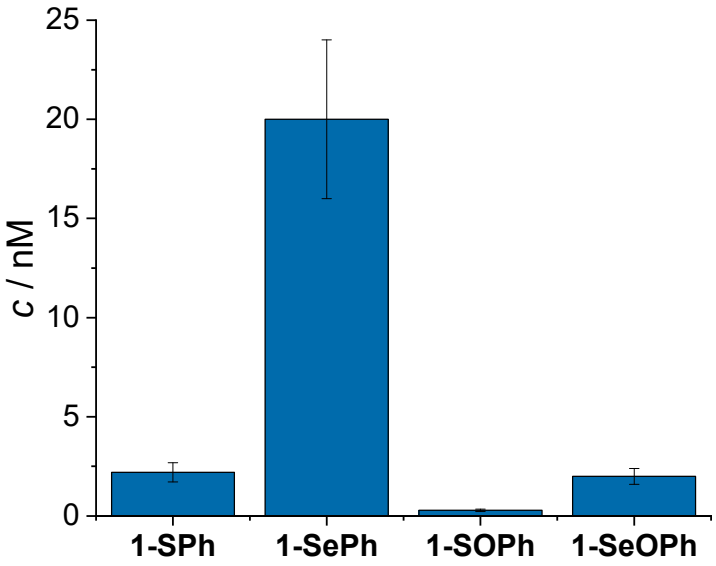

Figure S48. Limits of detection of **1-SPh**, **1-SePh**, **1-SOPh**, and **1-SeOPh** in methanol.

Ratiometric Fluorescence Detection

The mixtures of different molar fractions of (**1-SPh** + **1-SOPh**) and (**1-SePh** + **1-SeOPh**), respectively, were evluated by fluorescence spectroscopy. The fluorescence response was followed at 500 nm for the oxidized sensors and at 700 nm for their reduced counterparts. The ratio of fluorescence intensities at 700 and 500 nm is shown in Figure S49a,c, and the fluorescence spectra of pure forms are shown in Figure S49b,d.

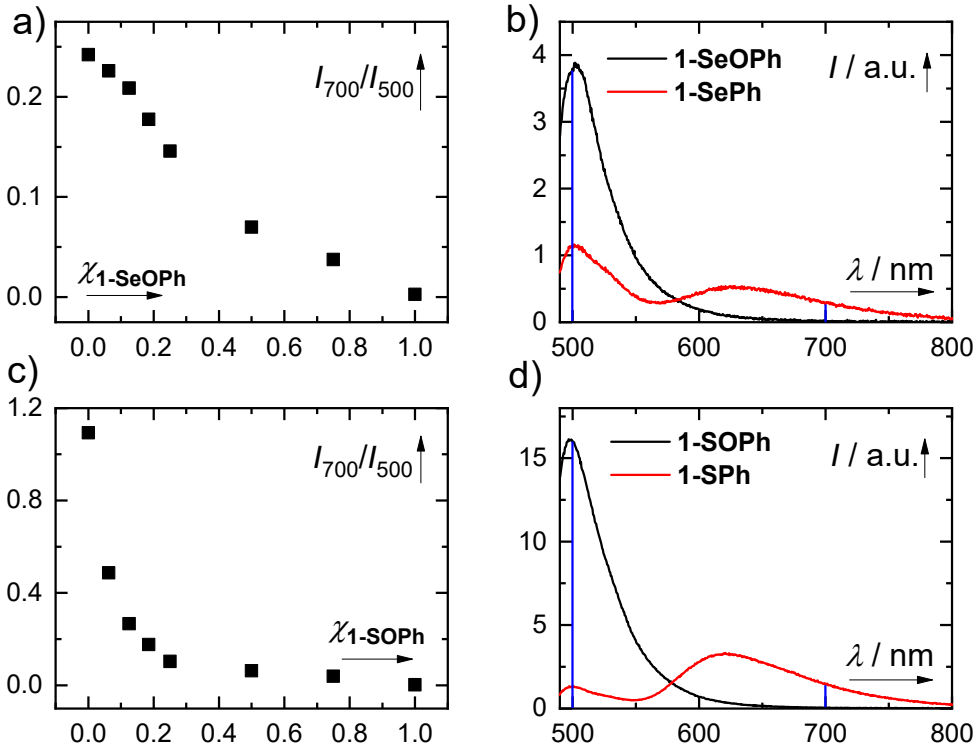

Figure S49. a) Ratio of the fluorescence signals at 700 and 500 nm for mixtures with various molar fraction of **1-SeOPh** in the presence of **1-SePh**. b) Fluorescence spectra of pure **1-SeOPh** and **1-SePh**. c) Ratio of the fluorescence signals at 700 and 500 nm for mixtures with various molar fraction of **1-SOPh** in the presence of **1-SPh**. d) Fluorescence spectra of pure **1-SOPh** and **1-SPh**. All spectra were measured in methanol at the excitation wavelength of λ_{exc} = 475 nm. Blue vertical lines in b) and c) indicate the fluorescence intensities at 500 and 700 nm.

References

1. Anshori, J. A.; Slanina, T.; Palao, E.; Klán, P. *Photochem. Photobiol. Sci.* **2016**, *15* (2), 250–259.
2. Palao, E.; Slanina, T.; Klán, P. *Chem. Commun.* **2016**, *52* (80), 11951–11954.
3. Rossi, R.; Bellina, F.; Mannina, L. *Tetrahedron* **1997**, *53* (3), 1025–1044.
4. Reich, H. J.; Renga, J. M.; Reich, I. L. *J. Am. Chem. Soc.* **1975**, *97* (19), 5434–5447.
5. Aston, N. M.; Robinson, J. E.; Trivedi, N. WO2007045861.
6. Palao, E.; Duran-Sampedro, G.; de la Moya, S.; Madrid, M.; García-López, C.; Agarrabeitia, A. R.; Verbelen, B.; Dehaen, W.; Boens, N.; Ortiz, M. J. *J. Org. Chem.* **2016**, *81* (9), 3700–3710.
7. Kim, J.; Kim, Y. *Analyst* **2014**, *139* (12), 2986–2989.
8. Makukhin, N.; Nosek, V.; Míšek, J. *Synthesis* **2018**, *50* (4), 772–777.